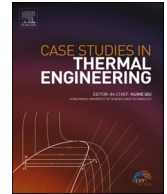




ELSEVIER

Contents lists available at ScienceDirect

## Case Studies in Thermal Engineering

journal homepage: [www.elsevier.com/locate/csite](http://www.elsevier.com/locate/csite)

# Exposure the role of hydrogen with algae spirogyra biodiesel and fuel-borne additive on a diesel engine: An experimental assessment on dual fuel combustion mode

S. Aravind<sup>a</sup>, Debabrata Barik<sup>a,b,\*\*</sup>, Gandhi Pullagura<sup>c</sup>, Sreejesh S.R. Chandran<sup>d</sup>, Elumalai PV<sup>1</sup>, Prabhu Paramasivam<sup>e</sup>, Dhinesh Balasubramanian<sup>f,\*</sup>, Yasser Fouad<sup>g</sup>, Manzoore Elahi M. Soudagar<sup>h,i,j</sup>, Md Abul Kalam<sup>k</sup>, Chan Choon Kit<sup>m</sup>

<sup>a</sup> Department of Mechanical Engineering, Karpagam Academy of Higher Education, Coimbatore, 641021, India

<sup>b</sup> Centre for Energy and Environment, Karpagam Academy of Higher Education, Coimbatore, 641021, India

<sup>c</sup> Department of Mechanical Engineering, GITAM School of Technology, Visakhapatnam, 530045, India

<sup>d</sup> Department of Mechanical Engineering, Mount Zion College of Engineering, Pathanamthitta, 689649, India

<sup>e</sup> Centre for Research Impact & Outcome, Chitkara University Institute of Engineering and Technology, Chitkara University, Rajpura, 140401, Punjab, India

<sup>f</sup> Department of Mechanical Engineering, Mepco Schlenk Engineering College, Sivakasi, Tamil Nadu, India

<sup>g</sup> Department of Applied Mechanical Engineering, College of Applied Engineering, Muzahimiyah Branch, King Saud University, Riyadh, Saudi Arabia

<sup>h</sup> College of Engineering, Lishui University, Lishui, 323000, Zhejiang, China

<sup>i</sup> Department of Mechanical Engineering, Graphic Era (Deemed to be University), Dehradun, Uttarakhand, 248002, India

<sup>j</sup> Division of Research and Development, Lovely Professional University, Phagwara 44411, Punjab, India

<sup>k</sup> School of Civil and Environmental Engineering, Faculty of Engineering and Information Technology, University of Technology Sydney, Ultimo, Sydney, NSW, 2007, Australia

<sup>1</sup> Department of Mechanical Engineering, Aditya University, Suarmpalem, 533437, India

<sup>m</sup> Faculty of Engineering and Quantity Survey INTI International University, Persiaran Perdana BBN, Putra Nilai, 71800, Nilai, Negeri Sembilan, Malaysia

## ARTICLE INFO

Handling Editor: Huihe Qiu

## Keywords:

Dual fuel

Hydrogen

Di-tert butyl peroxide

Algae residual carbon nanoparticles

Spirogyra biodiesel

Energy efficiency

## ABSTRACT

This investigation is focused on the study of the overall performance of a single-cylinder diesel engine with the use of 99.99 % pure elemental hydrogen (H<sub>2</sub>), as a gaseous fuel and algae Spirogyra biodiesel 30 % (SBD30) with 1.5 % Di-tert Butyl Peroxide (1.5%DTBP) as cetane improver and 2 % Algae Residual Carbon Nanoparticle (2%ARCNP). During the investigation, the hydrogen flow rate was controlled by an electronic gas injector and varied in the range of 5–20 lpm in the increment of 5 lpm. Among the fuel blends SBD30 + 1.5%DTBP+2%ARCNP+15H<sub>2</sub> acted as a good combination to reduce ID and CD; and to boost HRR, BTE, and EGT. Additionally, this resulted in a drastic decline in the emission components such as HC, CO, and smoke. However, a surge in NO was observed for all the fuel sampled by the induction of H<sub>2</sub>. For SBD30 + 1.5%DTBP+2%ARCNP+15H<sub>2</sub> a shorter ID and CD were observed at 7.2°CA and 34.5 °CA than diesel respectively at full load. The MCP for SBD30 + 1.5%DTBP+2%ARCNP+15H<sub>2</sub> was 81 bar which occurred at 9.2°CA, however, the HRR was 61.3 J/°CA which was 1.2 % lower than that of 20 LPM hydrogen flow rate, at full load respectively. By using hydrogen + DTBP + ARCNP, the BSFC was overall lower by about 22 % and the BTE was improved by about 36.1 %. The CO, HC,

\* Corresponding author.

\*\* Corresponding author.

E-mail addresses: [debabrata93@gmail.com](mailto:debabrata93@gmail.com) (D. Barik), [dhineshbala91@mepcoeng.ac.in](mailto:dhineshbala91@mepcoeng.ac.in) (D. Balasubramanian).

<https://doi.org/10.1016/j.csite.2024.105566>

Received 3 June 2024; Received in revised form 17 November 2024; Accepted 24 November 2024

Available online 26 November 2024

2214-157X/© 2024 The Authors. Published by Elsevier Ltd. This is an open access article under the CC BY-NC license (<http://creativecommons.org/licenses/by-nc/4.0/>).

and smoke for SBD30 + 1.5%DTBP+2%ARCNP+15H<sub>2</sub> was 64.8 %, 38.8 %, and 29.2 % lower than diesel however, the NO emission was 32.6 % higher than diesel at full load respectively.

## Nomenclature

CO	–	Carbon monoxide
CO <sub>2</sub>	–	Carbon dioxide
H <sub>2</sub>	–	Hydrogen
BSFC	–	Brake-Specific Fuel Consumption
NO	–	Nitrous Oxide
CI	–	Compression-Ignition
SBD	–	Spirogyra Biodiesel
DTBP	–	Di-tert Butyl Peroxide
ARCNP	–	Algae Residual Carbon Nanoparticle
IP	–	Injection Pressure
CR	–	Compression Ratio
HRR	–	Heat Release Rate
CA	–	Crank Angle
MCP	–	Maximum Cylinder Pressure
ID	–	Ignition Delay
CD	–	Combustion Duration
BTE	–	Brake Thermal Efficiency
NO	–	Nitrogen Oxide
HC	–	Hydro Carbon
MEA	–	Methoxyethyl Acetate
HHO	–	Oxy-hydrogen gas
a TDC	–	After Top Dead Center
b TDC	–	Before Top Dead Center
a BDC	–	After Bottom Dead Center
b BDC	–	Before Bottom Dead Center
CV	–	Calorific Value
EGT	–	Exhaust Gas Temperature
SC	–	Single Cylinder
DF	–	Dual Fuel
KV	–	Kinematic Viscosity
IT	–	Injection Timing
BP	–	Brake Power

## 1. Introduction

Diesel engines are more reliable, sufficient, and fuel-efficient, hence adopted in transportation, locomotives, maritime, power generation, earth-moving gadgets, and agriculture due to its power [1,2]. But the high prices of petroleum products, diminishing reserves of fossil fuel, causing more environmental pollution has brought the necessity for other fuel sources to notice. Renewable energy, especially biofuels, is under the spotlight as sustainable and eco-friendly alternatives to the conventional fossil fuels. Biodiesel from different feedstocks, such as algae, animal fats, and vegetable oils, is known to comprise long-chain monoalkyl esters. Biodiesel may replace or at least blend with diesel fuel originating from petroleum [3]. They have other advantages, such as neatness and stability, less green house gas emissions, large lubricity, or safety etc. The high production costs in addition to poorer performance and higher NO<sub>x</sub> emissions in comparison to petroleum diesel are some of the constraints faced. Some low-cost feedstocks such as algae now find part of the answer to the problem of sustainably produced biodiesel with much lower cost while affording oil. Research is being directed towards understanding alternatives including changes in the geometries of engines, modified EGR, and alternate formulations concerning the fuels to enhance the performance and reduce the emissions from engines. Out of these alternatives, the most efficient amongst all those methods that have been implemented for enhancing the combustion and the overall performance of the engine, it is fuel reformulation.

Algae are found in aqueous environments and sequester CO<sub>2</sub> using solar energy to convert it into biomass. They are categorized into two subclasses, namely microalgae and macroalgae. Microalgae are unicellular, minute and suspended in water, while macroalgae are large, multicellular organisms and are present in ponds; an example of macroalgae is seaweed. Microalgae grow many times faster than terrestrial plants and accumulate more fat, some of them containing fatty acid content reaching 70 %, which is the primary reason they are utilized in biodiesel production. Algal biomass has three main fractions, triglycerides, carbohydrates, and bio-proteins, among which oils are produced from triglycerides and can be converted into biodiesel. The triglyceride oils can be converted into biodiesel that can be used as fuel in generators [4]. Microalgae have several advantages over other feedstocks like easy to grow, and they produce eight to ten times more oil than terrestrial crops. The oil content in algae varies in between 20 % and 50 %, and some species, for example, *Botryococcus braunii*, can have up to 80 % oil content. The estimated oil production in algae is around 100,000 L per hectare per year just from the third of France [5]. Algae are considered the most promising source of biomass due to rapid growth rates and high biofuel yields (2000–5000 gallons per acre annually), efficient CO<sub>2</sub> consumption and O<sub>2</sub> release and noncompetitive with

agriculture for land or food for energy production. The *Spirogyra* genus, folk as pond silk, belongs to the Zygnematales class and includes about 400 genera, that predominantly live in freshwater. They form long unbranched chains in a row, because the algae can float in the water, can float. The protein and the silica that link the cells, and the gas produced when the photosynthesis is made will float the algae, which explains why these algae can float. The following picture usually shows thousands of silica on the surface of these algae, the surface of the fine lines of the set is connected. PdfPCell 8. Utilization of *Spirogyra* algae for biodiesel production, which ESA supports is the remedying of the spilled oil in the sea.

The use of a single-cylinder diesel engine with a dual fuel system allows high-efficiency blending of hydrogen and biodiesel-diesel fuels which significantly resolves associated environmental concerns, fuel savings, and decreased reliance on conventional diesel. Hydrogen is employed as the secondary fuel required to achieve clean combustion and emissions, contributing to the development of sustainable and eco-friendly diesel engine technologies. For instance, Uludamar et al. (2018) [6] employed microalgae biodiesel and diesel in an HCCI hydrogen-fueled combustion mode and concluded through their study that there was a decrease in brake power and torque with microalgae biodiesel, while the use of hydrogen is very effective in generating reductions in CO and NO<sub>x</sub> emissions in both HCCI and CI-turbulence aided modes. Similarly, Sharma et al. (2022) [7] looked at the influence of ternary mixture of fuel to power the engine with hydrogen peroxide as an additive to improve the engine performance. Results of tests showed that B20H10 generated the best ones. While lowering BSFC through 7.98 %, CO and HC emissions through 26.5 %, and 6.67 %, correspondingly, B20H10 increased BTE by 6.56 % and HRR by 8.5 %, compared to B20. Kumar et al. (2023) [8] reviewed the recent development in hydrogen enrichment with microalgae biodiesel for internal combustion engines. The review highlighted the wide flammability limits and flame propagation rate at a lean mix of hydrogen, which makes it an ideal replacement blended with third-generation biofuel microalgae biodiesel.

Mohite et al. (2024) [9] assessed pilot fuel, injection parameters (IPs), and engine loads influencing the performance and emissions of dual-fuel engines utilizing algae biodiesel and hydrogen. Their optimization studies reflected a positive trend in brake thermal efficiency (BTE) along with diminished CO, hydrocarbons (HCs), and soot emissions. Further, Mohite et al. (2024) [10] attempted to optimize injection timing (IT) and engine loading by response surface methodology to improve dual-fuel engine performance with hydrogen and biodiesel. This application had an extensive reduction in emissions while keeping comparable to BTE along with a higher liquid charge replacement ratio. Annamalai and Murugesan (2024) [11] studied the efficiency and emissions of a CI engine fuelling hydrogen and algae-derived biodiesel by varying H<sub>2</sub> substitution rates. They demonstrated an enhancement of 1.92 % in BTE and 9.5 % reduction in brake-specific fuel consumption (BSFC) for maximum load compared to diesel, while emissions of NO<sub>x</sub> were increased by 18 %. Because of this, there is a significantly reduced quantity of UHC, CO, and smoke emissions, which suggests that biodiesel from algae with hydrogen improves efficiency and reduces emissions. Sindhu et al. (2024) [12] have studied the biodiesel conversion of *Botryococcus braunii* microalga oil mostly focusing on how hydrogen infusion has worked for a diesel engine's efficiency, combustion, and emissions. The study concluded that hydrogen-enriched biodiesel achieved satisfactory levels of engine torque and thermal efficiency with decreased harmful emissions, depicting this green fuel as a wonder renewable alternate to fossil fuel.

Numerous researchers have tried to combine nanoparticles with biodiesel-diesel mixtures and further introduce hydrogen combustion to enhance performance and decrease emissions during the process of enhancing performance and reducing emissions. Nanoparticles enhanced fuel properties due to their high surface area-to-volume ratio and their unique thermal and electrical characteristics. Being energy carriers, they enhance the transfer of heat and reduce ignition delay, thus lowering pollution by reducing CO, UHC, CO<sub>2</sub>, and NO<sub>x</sub> levels. For example, Xia et al. (2021) reported increases in brake thermal efficiency by about 2 % along with decreased emissions when 50 ppm Al<sub>2</sub>O<sub>3</sub> nanoparticles were added to castor oil methyl ester at higher loads. Tosun and Özcanli reported better engine performance and fewer emissions with aluminium oxide when used in a diesel-soybean biodiesel-hydrogen blend. Manigandan et al. have shown that the TiO<sub>2</sub> nanoparticles caused the braking power to increase by 22 %, while ZnO elevated it by 4 %, accompanied by impressive drops in the corresponding emissions. Chetia et al. explored introducing hydrogen and CeO<sub>2</sub> nanoparticles into waste-frying palm biodiesel and found a 3.53 % increase in brake thermal efficiency and a 16.12 % reduction in brake-specific fuel consumption, with an 11 % increase in NO<sub>x</sub> emissions. This blend is a candidate and a good alternative to fossil fuels for improved efficiency and properties.

There have been limited studies on alcohols in biodiesel-diesel blends incorporated into hydrogen dual-fuel engines. Alcohols derived from renewable sources are highly oxygenated, having high latent heat of vaporization, contributing to combustion efficiency and lowering cylinder temperature and NO<sub>x</sub> emissions. However, these alcohols are hydrophilic, resulting in instability, high auto-ignition temperatures, poor lubrication, lower cetane indices, engine modifications, and corrosion issues that limit their application to a 5–10 % mixture level. Rajak et al. (2020) [13] studied the effect of H<sub>2</sub>-enriched diesel, *Spirulina* microalgae, n-butanol, and diethyl ester fuels on diesel engine performance and emissions. The study results showed that, in comparison with biodiesel-diesel, H<sub>2</sub> increased BTE, reduced BSFC, and curtailed emissions of CO<sub>2</sub> and smoke, although NO<sub>x</sub> emission increased. Chaurasiya et al. (2022) [14] found lower emissions and steady BTE with n-butanol even with 5 % hydrogen, DEE, and n-butanol domain as a blend in *Spirulina* microalgae biodiesel-diesel. Barik et al. (2024) [15] used DDEE mixtures with H<sub>2</sub> as the secondary fuel and discovered that the DDEE<sub>20</sub>+H<sub>2</sub> blend yielded the best results in the production of increased mean cylinder pressure and rate of heat release (HRR), enhanced BTE, and diminished emissions despite a little rise in NO<sub>x</sub>. Kumar et al. (2021) [16] examined the use of Di-tert Butyl Peroxide (DTBP) as an additive (1–5%) in diesel with 40 % H<sub>2</sub>. The authors reported that DTBP at 4 % reduced NO<sub>x</sub> emissions at all loads, and 5 % DTBP abated CO emissions by 69 % at a load of dual-fuel operation.

The study by Al-Dawody et al. (2022) pointed out that although biodiesel derived from *Cladophora* and *Fucus* algae lowered the emission of NO<sub>x</sub> and soot, it had negative impacts on thermal efficiency, and overall increased fuel consumption [17,18]. Therefore, exploring the conversion technology of algae is significant for its potential as a renewable energy source. Algae, In hydrothermal liquefaction experiments Jazie et al. (2022) investigated the hydrothermal liquefaction of *Fucus vesiculosus* algae, reported that the

energy value of crude oil produced at 300 °C with a zeolite catalyst was 38.47 kJ/kg, [19]. In another topology, Al-Dawody et al. (2023) examined dual-fuel diesel engines operating on the diesel-ammonia-water emulsion, shows an 80 % reduction in NO<sub>x</sub> and soot emissions but the engine performance deteriorated with the decrease in the heating value of ammonia [20]. Murad and Al-Dawody, 2022 compared the characteristics of the engine with AME biodiesel blends which concluded a decrease in cylinder pressure and emission of SO<sub>2</sub> but a decline in BTE and a rise in BSFC [21,22]. The effects of different biofuels were investigated in a turbocharged diesel engine by Hamza et al. (2023), indicating that while biofuels reduce peak cylinder pressure and NO<sub>x</sub> emissions, they require a higher engine BSFC [23,24]. All of these studies together suggest that further use of biofuel and other additives to fuel can improve performance and decrease emissions, although not necessarily without the cost of efficiency and amount of fuel used.

### 1.1. Research gap and objectives

From the above literature survey, it is found that the addition of hydrogen along with a biodiesel-diesel mix enhances the engine's overall performance parameters. However, the addition of nanoparticles and cetane improvers also boosts performance and diminishes emissions. In the present work, ARCNP is a nanoparticle that was produced from natural algae residuals (a waste after extraction of methyl ester from *Spirogyra*) which includes pigments, minerals, proteins, polyunsaturated fatty acids, and carbohydrates. The prepared algae nanopowders of 2 % were mixed with SBD30 to prepare the blend. In addition to this, the use of hydrogen in CI engines usually causes ID, because of its high-octane rating, when used in CI engines. To counter this, DTBP is a cetane improver and an oxidation booster, being an organic compound used at 1.5 % concentration to reduce the ID during dual fuel operation of the modified engine. Because no research has been conducted with the addition of algal residual carbon nanoparticles and cetane improver in algae biodiesel-diesel blends and H<sub>2</sub> enrichment. Hence, the current study seems to be novel and informative to evaluate the effect of algae nanoparticles, with the aid of a cetane booster and with H<sub>2</sub> infusion to determine the overall combustion, performance, and emission parameters of a dual fuel engine.

## 2. Materials and methodology

### 2.1. Fuel preparation

#### 2.1.1. Algae oil extraction

The algal oil from the species of *Spirogyra* was extracted using the Soxhlet extraction method with n-hexane as the solvent. The *Spirogyra* algae were grown in a water tank of Karpagam Academy of Higher Education, sun-dried, and powdered by a mechanical grinder to fine powder. The harvested algae were strained through a round metal grid with various grid sizes of different average powder sizes; for example, with 30- $\mu$ m mesh, the average was at 0.366  $\mu$ m; for 40- $\mu$ m mesh, it was 0.462  $\mu$ m; and for 60- $\mu$ m mesh, it was 0.641  $\mu$ m. Standard n-hexane provided by a dealer in the locality was used for the extraction in the Soxhlet apparatus at 750 ml in volume. The algae powder was filled into a thimble provided with filter paper and the extraction was carried out following the experimental design. At the end of each experiment, the oil was separated from the oil-solvent mixture by distillation heating to 75 °C corresponding to the boiling point of n-hexane.

#### 2.1.2. Algae biodiesel

In the present investigation, algae biodiesel was used as liquid fuel produced from algae *spirogyra*. The *spirogyra* oil extraction methodology has been explained in the earlier section 2.1.1. The *spirogyra* biodiesel (SBD) was produced from the *spirogyra* algae oil, with calcined quail egg shells being a heterogeneous catalyst used in the transesterification process. Before the SBD production process,

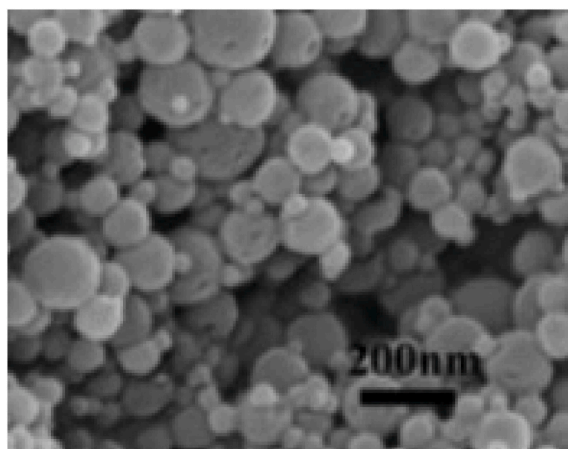


Fig. 1. Sem image of ARCNP

spirogyra bio-oil was extracted from the Spirogyra algae and then mixed with methanol inside a reaction vessel. Subsequently, the calcined quail eggshell catalyst was added into the reaction vessel where the mixture had been set under a temperature of approximately 60–70 °C to facilitate the transesterification reaction. During this stage, the triglycerides found in the algae bio-oil reacted with methanol to produce FAME and glycerol as a by-product. The reaction was allowed to take place for a given period; afterwards, the reaction mixture was left to settle, thereby separating the biodiesel phase from the glycerol and catalyst residue. The washed and dried biodiesel purification process thus shows potential as renewable and sustainable energy.

### 2.1.3. ARCNP preparation

The extracted oil from algae of the genus Spirogyra was processed using the Soxhlet method to further process the residual algae powder into ARCNP. The residue was pyrolyzed to carbon the said residue and ground in a mechanical ball mill for size reduction to the nanolevel. The particles were examined by a particle analyzer to meet the nanoscale grade. A surfactant of lipophilic type non-ionic surfactant (QPAN80) was added to stabilize the nanoparticles within the SBD30 blend. The stability of the fuel blend with ARCNP addition was ensured by using zeta potential analysis.

### 2.1.4. Characterization of ARCNP

The characterizations of ARCNP in this study involved several techniques. Fig. 1 shows the SEM image of the ARCNP. With the use of SEM, the surface morphology of the nanoparticles was studied to understand their flow friction during its flow in the injector nozzle blended with SBD30 and DTBP. It is observed the smooth morphology of the ARCNP may offer streamlined flow without creating flow barrier and backpressure in the injector. SEM observations also indicate that ARCNP has porous structures and even surface morphology, thus offering vast surface areas ideal for the burning of fuel as well as effectiveness in catalytic reactions. The roughly spherical particles with partial aggregation provide an ideal shape for uniform dispersion in the biodiesel matrix due to their morphological characteristic. The configuration may also enable better fuel atomization and combustion. The nanoscale size of ARCNP ensures that they act as efficient catalysts, optimizing the interaction between biodiesel and hydrogen, thereby possibly improving energy output, decreasing emissions, and enhancing fuel efficiency in biodiesel engines.

Fig. 2 shows the TGA analysis for ARCNP. TGA analysis was carried out to understand the thermal stability of ARCNP particles. Because, when a fuel blend such as SBD30-DTBP-ARCNP is injected into the combustion chamber, that time for combustion is much less hence in the short interval time, the ARCNP should take part in the combustion and degrade thermodynamically. It is also observed that a rapid thermal degradation happened to ARCNP at a temperature after 598 °C. This indicates the effective participation of ARCNP in the combustion process creating multiple combustion centers in the combustion chamber. In the first degradation step a weight loss of 2.35 % between 24.7 °C and 105.4 °C was observed, which may be due to moisture or volatiles being released. There is also a small weight change of 0.65 % which occurs between 108.4 °C and 231.8 °C probably due to the removal of some organics that are not tightly held. Weight loss of 8.55 % is noted between 231.8 °C and 408.0 °C, which shows destruction of organic matter, and then 3.66 % loss from 408.0 °C to 598.1 °C, revealing additional organic matter breakdown. The highest loss which is 35.91 % occurs in the range of 598.1 °C and 799.4 °C and is due to decomposition of carbon components with the sample retaining a mass of 48.87 % at 799.4 °C.

Fig. 3 indicates the XRD for the ARCNP. XRD analysis indicates the crystalline structure of the ARCNP. From the graph, it is observed that the XRD result for the ARCNP sample indicates the existence of crystalline material, which has several peaks. Its sharp and profound peaks are at 2-theta values of 22.94°, 29.33°, 35.93°, 39.37°, and 43.15°, corresponding to some crystallographic planes. The highest peak at 29.33° of intensity with 8506 counts appears to be the principal plane, while two other high-intensity peaks at 39.37° and 43.15° represent the contribution of the secondary plane. The steepness and intensity of these peaks verify that the sample is relatively crystalline with moderate amorphous content.

The FTIR analysis for the ARCNP is shown in Fig. 4. FTIR indicates the surface functional group and type of bonds in the ARCNP molecules. The FTIR spectrum of ARCNP reveals the existence of some fundamental absorption peaks which can be used to understand more about its molecular structure. The absorption around 1643.35 cm<sup>-1</sup> suggests carbonyl (C=O) stretching vibrations; the peaks at

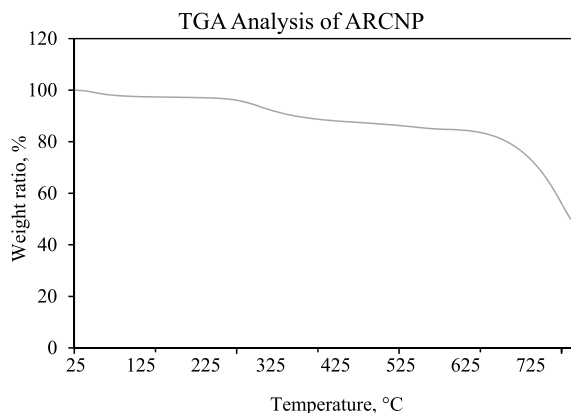


Fig. 2. TGA of ARCNP

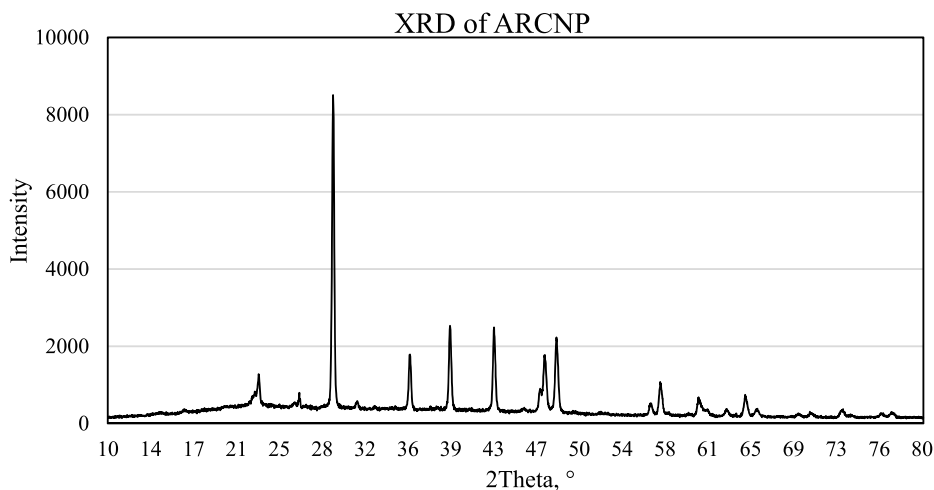


Fig. 3. Xrd analysis of ARCNP

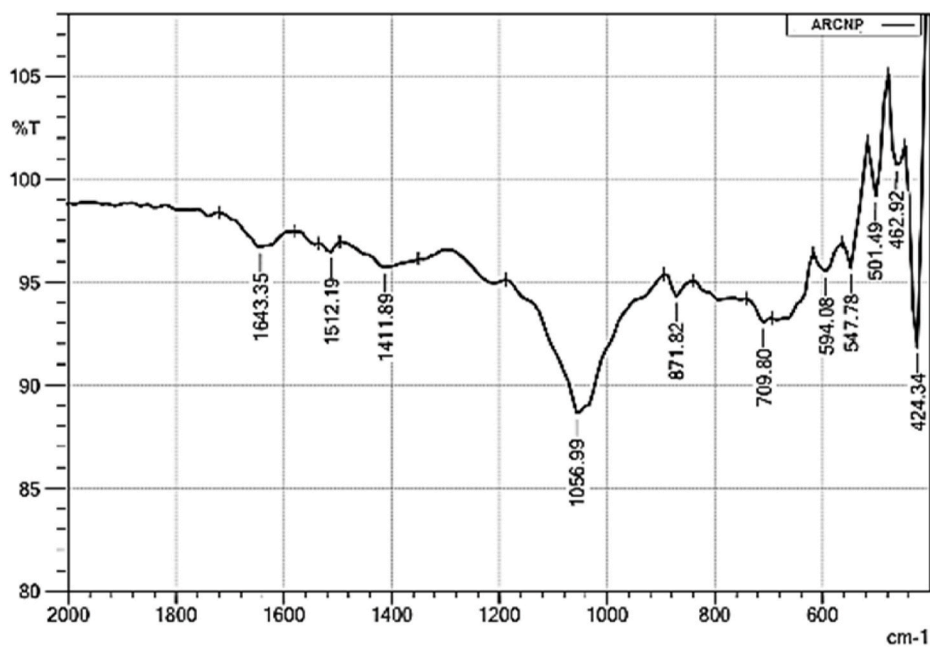


Fig. 4. FTIR of ARCNP

1512.19  $\text{cm}^{-1}$  and 1411.89  $\text{cm}^{-1}$  are attributed to C=C aromatic ring stretching. The most intense peak at 1056.99  $\text{cm}^{-1}$  can be attributed to C-O stretching. The labeled peaks within the range of 817.82  $\text{cm}^{-1}$  and 462.92  $\text{cm}^{-1}$  may perhaps be categorized under out-of-plane bending vibrations, hence providing more information on structural units of ARCNP.

Table 1

Physiochemical properties of diesel and other prepared blends.

Properties	ASTM STD	Pure Diesel	SBD30	SBD30 + 1.5%DTBP+2%ARCNP
Density at 15 °C ( $\text{Kg}/\text{m}^3$ )	D 4052	822.8	844.65	842.3
CV ( $\text{MJ}/\text{kg}$ )	D 4809	45.75	44.39	61.87
KV at 40 °C, ( $\text{mm}^2/\text{s}$ )	–	4.03	4.123	3.79
Flashpoint (°C)	D 93	52	65	64.8
Cetane number	D 613	49	50.6	57.31

### 2.1.5. Properties of blended fuel

Tables 1 and 2 compare fuel characteristics based on ASTM standards for pure diesel, and spirogyra biodiesel-diesel (SBD) blends with a constant concentration of 1.5 % of Di-tert-butyl peroxide (DTBP) and 2 % of Algae Residual Carbon Nanoparticles (ARCNP) and H<sub>2</sub> (at a flow rate of 5, 10, 15, and 20 lpm). The first table lists the physiochemical properties of diesel and various SBD blends including density at 15 °C, calorific value (CV), kinematic viscosity (KV) at 40 °C, flash point, and cetane number. The first blend includes 30 % of Spirogyra biodiesel and 70 % of diesel and is termed SBD30. The remaining blends includes SBD30, a fixed concentration of 1.5 % of DTBP, a constant quantity of 2 % of ARCNP, and H<sub>2</sub> enrichment at a flow rate of 5, 10, 15, and 20 lpm and these blends are referred as SBD30 + 1.5%DTBP+2%ARCNP+5H<sub>2</sub>, SBD30 + 1.5%DTBP+2%ARCNP+10H<sub>2</sub>, SBD30 + 1.5%DTBP+2%ARCNP+15H<sub>2</sub>, SBD30 + 1.5%DTBP+2%ARCNP+20H<sub>2</sub> respectively. The physicochemical properties of H<sub>2</sub> are mentioned in Table 2.

### 2.2. Hydrogen injection setup and approach

The setup comprises a hydrogen cylinder with safety mechanisms, flow meters, and a very accurate injection system using a five-hole solenoid-based computerized injector [25]. The hydrogen cylinder has flame trappers and arresters to guarantee safety during handling and injection. Flame trappers block flames from entering the cylinder, while flame arresters are designed to extinguish any fire that could reach the hydrogen source. This safety element is essential when handling extremely combustible hydrogen gas. A flow meter is employed to quantify the amount of hydrogen pumped into the engine. The injection approach employs separate high-pressure pumps for hydrogen functioning at 5 bar pressure. The injection is carried out near the intake valve utilizing a highly advanced electronic injector with a solenoid mechanism and five separate holes. Every hole has a nozzle diameter of 0.126 mm. The injection process is regulated using a microcontroller, specifically the Atmega-328. The microcontroller is configured to govern the injection amount of hydrogen (H<sub>2</sub>) using PWM. The duty cycle of PWM modulates the injection quantity according to user-defined parameters. An L293D adapter is employed to supply the required power to the injector unit, pump, and microcontroller unit. This component is responsible for ensuring accurate power distribution and synchronization between the different components of the injection system. The injection technique is closely linked to the precise engine valve timing and speed coordination. Upon analyzing the valve timing values, it is evident that the intake valve remains open for 220 °CA relative to the crankshaft's position. During the valve overlap period of 9 °CA, both the intake and exhaust valves are in an open position. The duration of this intake is effectively lowered to 211 °CA. The programming of the microcontroller is customized to introduce H<sub>2</sub> and DTBP at precise angular intervals throughout the engine cycle. This results in three equal angle injection lengths of 70.3 °CA each out of the 211 °CA effective ingestion duration. The microprocessor is programmed to commence injection at specific intervals, 70.3 °CA, 140.6 °CA, and 210.9 °CA, to optimize the fuel-air combination for enhanced combustion efficiency. Hydrogen is highly combustible as compared to other alternative alternatives such as CNG, LPG, and biogas [26]. Hydrogen is not readily available in nature, but it occurs in all renewable sources and may be produced by fuel cells utilizing biomass, water, natural gas, solar, and wind. Hydrogen has recently gained popularity since it plays an important role in numerous applications, including power production, industry, and transportation. Hydrogen has a higher calorific value of 124 MJ/kg and a higher cetane number, allowing for better power output in internal combustion engines, but it is more challenging to store and handle [27]. H<sub>2</sub> is an excellent choice for SI engines due to its acceptable physiochemical characteristics. However, in CI engines, it is employed as a supplementary fuel [28].

### 2.3. Engine setup

The experimental setup features a dual-fuel, single-cylinder, CI engine. For engine loading an eddy current-type dynamometer was employed in this study. The engine Schematic layout and actual engine setup are depicted in Figs. 5 and 6. The engine is capable of adjusting the compression ratio continuously via engineered moving chamber blocks without altering ignition chamber calculations. Crucial equipment measures the crank angle and combustion pressure, are linked to a computer for Pθ–PV chart creation. Equipment for air and fuel flow rate, temperatures, and load measurement is integrated, including manometers and transmitters. An independent panel box houses equipment like air boxes and fuel tanks for dual fuel tests. A system for hydrogen and cetane booster injection, controlled by a PLC, is also incorporated. Flow rates of water used for cooling and calorimeter water are measured by rotameters. Real-time performance evaluation is enabled by Lab View-powered software called "IC Engine soft" which allows comprehensive monitoring and analysis of engine performance metrics during testing. This setup, combined with the software, forms an advanced platform for thorough investigation and assessment of test engine performance. It was deployed in the engine setup that each instrument was validated and calibrated in reference with the earlier studies. The gas analyzer was zeroed with standard gas mixtures with

**Table 2**  
Physiochemical properties of H<sub>2</sub>.

Properties	ASTM	H <sub>2</sub>
Octane number	D 2699	135
Density, kg/m <sup>3</sup>	D 3588	0.087
Autoignition Temperature, °C	–	620
CV, MJ/kg	D 1945	145.36
Flashpoint, °C	–	–253
Fire point, °C	–	–241
Purity, %	D 7941	99.99

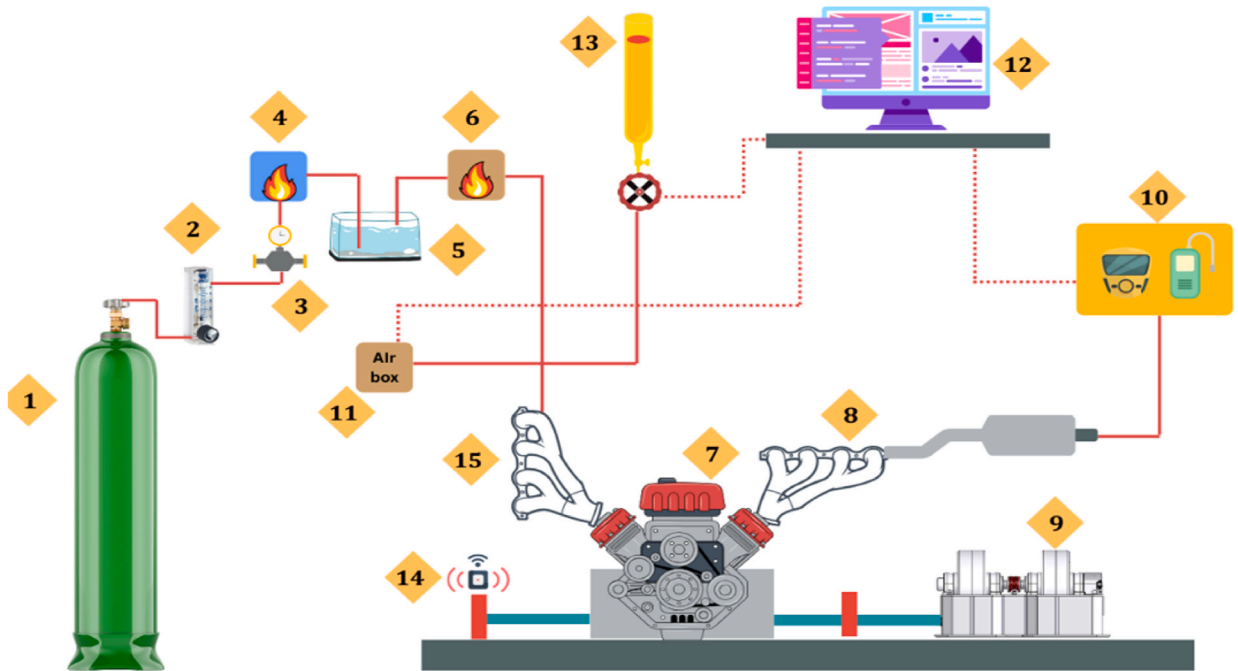


Fig. 5. Engine layout.

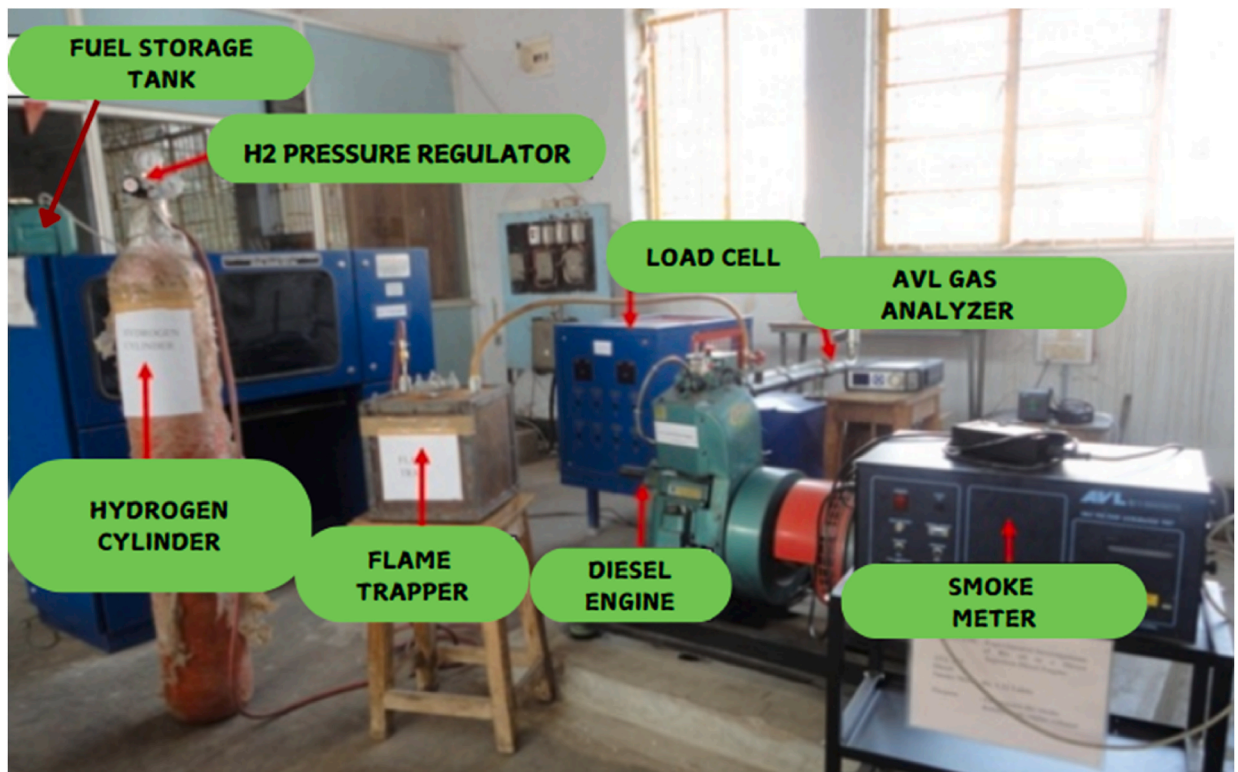


Fig. 6. Engine test setup.

concentration quantified to obtain accurate emissions data, the methods employed by Pullagura et al. [27]. To obtain high precision in the torque and power collected from the dynamometer, the dynamometer was calibrated with known weights as done in Vijayaragavan et al. [29]. For effective determination of crank angle, the crank angle encoder was placed adjacent to the Top Dead Center (TDC) of the crankshaft. The speed sensor was tested in relation to a tachometer to try to ascertain that the speed was measured accurately. The function of the smoke meter was calibrated using a clean air filter and standard smoke value; thus, having fixed particulate for comparison as used in Bora et al. [30]. To maintain calibration of the burette, known volumes of liquid were used to get accurate measurement of fuel and fluid. Finally, the pressure transducer was calibrated with the help of pressure calibration pump to ensure the accuracy of pressure transducer in different pressure level but similar to previous study [26,27,29,30]. Table 3 shows the complete specification of the test engine. The instruments and error details are given in Table A1.

## 2.4. Engine combustion, performance, and emission parameters

### 2.4.1. Engine combustion characteristics

Ignition delay (ID) is the period from when fuel injection begins to when combustion starts. It is essential in influencing combustion efficiency and emissions. Extended ID can result in either premature or delayed combustion. The combustion duration (CD) refers to the period in which the fuel combusts in the combustion chamber. It impacts the power generation, effectiveness, and emission rates. Efficient energy release is achieved through the ideal duration of combustion. The cylinder Pressure plotted against the CA graph depicts the changes in pressure within the cylinder during the engine cycle. The tool offers information on combustion efficiency and peak pressure and assists in optimizing fuel injection timing (IT) for peak power output. The HRR represents the speed at which energy is emitted during the process of combustion. It assists in comprehending the mechanics of the combustion process, aids in optimizing fuel injection techniques, and impacts engine performance.

**2.4.1.1. Ignition delay.** Ignition delay is the time from the start of injecting fuel into the cylinder up to the point where ignition occurs, and this plays a vital role for determining engine efficiency, power, and emissions. It consists of two distinct phases such as physical delay and chemical delay. The physical delay phase is characterized by the period for the fuel droplets to atomization, and mix with the air, and get volatilized and make ready for start of ignition. These processes enable the fuel to create a vaporized and homogenised air-fuel mixture for good combustion. After this phase, the second phase is the chemical delay where the reactions begin to the fuel air mixture. At this stage heat is absorbed from the combustion chamber air and creates free radicals resulting from pre ignition reactions. During these reactions the mixture reaches the state of auto ignition resulting in a rapid and sustained combustion. It is also understand that physical and chemical delay depends on fuel physiochemical properties, combustion chamber temperature, air pressure in the combustion chamber and injection time.

### 2.4.2. Performance attributes

BSFC is a metric that gauges the fuel efficiency of an engine. It denotes the fuel consumption per unit of power generated. Decreased BSFC values correspond to improved fuel efficiency.

$$BSFC = \frac{FFR}{BP} \cdot \frac{g}{kWhr} \quad \text{---} \quad \text{eq(1a)}$$

BTE quantifies the engine's ability to transform fuel energy into mechanical work efficiently. Increased BTE readings indicate enhanced overall performance and energy efficiency.

$$BTE = \frac{BP \times 3600}{FFR \times CV} \times 100 \% \quad \text{---} \quad \text{eq(2)}$$

EGT indicates the amount of energy left in the exhaust gases following combustion. It is essential to monitor this parameter to avoid overheating and improve fuel-air ratios.

**Table 3**  
Engine specification.

Engine parameters	Specifications
<b>Model and make</b>	TV1 and Kirloskar
<b>No. of Cylinder</b>	One
<b>Bore × Stroke</b>	87.7 × 110 mm
<b>Principle of combustion</b>	Direct injection and compression ignition
<b>Capacity</b>	661 cc
<b>CR</b>	17.5
<b>Rated speed</b>	1500 RPM
<b>Fuel timing for std. engine</b>	23° bTDC
<b>Valve clearance inlet</b>	0.18 mm
<b>Valve clearance exhaust</b>	0.20 mm
<b>Bumping clearance</b>	0.046" – 0.052"
<b>Lubrication system</b>	Forced feed system
<b>Connecting rod length</b>	234 mm

2.4.3. Emission characteristics

CO emissions indicate incomplete combustion. Reducing CO emissions is crucial for environmental and health reasons.

$$CO = \frac{\left(\frac{m_f+m_{gf}+m_a}{29}\right) \times 10 \times CO \text{ (in \%vol)} \times 28}{BP} \text{ (g / kWh)} \text{ --- --- --- eq(3)}$$

HC emissions occur due to either unburned fuel or incompletely combusted HCs. Regulating HC emissions helps maintain air quality.

$$HC = \frac{\left(\frac{m_f+m_{gf}+m_a}{29}\right) \times 10 \times HC \text{ (in \%vol)} \times 13}{BP} \text{ (g / kWh)} \text{ --- --- --- eq(4)}$$

Nitrogen oxide emissions, particularly NOx, are linked to elevated combustion temperatures. Controlling NO emissions is crucial for compliance with environmental standards and minimizing air pollution.

$$NO = \frac{\left(\frac{m_f+m_{gf}+m_a}{29}\right) \times 10 \times NO \text{ (in \%vol)} \times 32.4}{BP} \text{ (g / kWh)} \text{ --- --- --- eq(5)}$$

Smoke emissions are a sign of incomplete combustion and the presence of particulate particles. Decreasing smoke emissions enhances air quality and guarantees adherence to emission regulations.

The major factors affecting NOx emissions in diesel engines are high combustion temperature, availability of excess oxygen, the time interval the combustion products spend at high temperature zones, and characteristics of the fuel. High combustion temperatures are primarily cause for NOx generation particularly when hydrogen is added to the fuel due to high combustion reactivity of H<sub>2</sub> promoting peak rise in temperature. In addition to this availability of oxygen molecules in biodiesel promotes the formation of NOx. During high temperature oxygen molecules and nitrogen molecules reacts and produces thermal NOx as a by-product. And another cause for NOx is due to longer time for combustion. During this consequence nitrogen and oxygen forge together to produce NOx. Usually biomass based fuels contains dissolved oxygen in it, which lead to elevated NOx emission during the combustion process.

2.5. Instrument error analysis

Every instrument, which is used in the setup of the engine testing, has certain measurement error, therefore, it is crucial to know how to eliminate them through error analysis. For instances, gas analyzer can develop problems with the sensors hence revealing wrong figures on emission from the exhaust while dynamometers can develop problems in determining the right torque or speed to produce the correct brake power. Crank angle encoders may contain signal delays that affect the crank position and, speed sensors may add latency errors when measuring engine speed. Smoke meters are interference sensitive and may read a wrong smoke opacity while burettes used in fuel consumption may encounter errors arising from manual reading as well as due to change in temperature. Pressure transducers used to measure in-cylinder pressure may also realise some difficulties due to temperature influence and dynamic character. If the errors are not calibrated or corrected, some of them must be eliminated for accurate and consistent testing of the engine.

The evaluations of the unknown unreliability of a measured physical quantities can be determined by using the general equation given below [15].

$$\frac{U_z}{Z} = \sqrt{\left[ \sum_{i=1}^n \left( \frac{1}{Z} \frac{\partial Z}{\partial x_i} \right)^2 \right]} \text{ --- --- --- (1b)}$$

The symbol Z on this equation is the physical quantity that is reliant on parameters xi and UZ stands for the type of uncertainty linked with Z. The measurement uncertainties for the instruments employed in the research were captured in the study's Table A1.

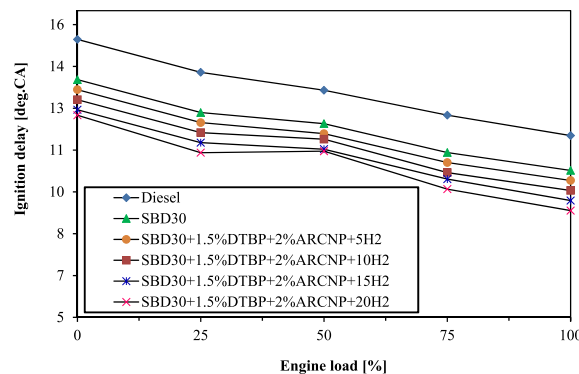


Fig. 7. ID vs Engine load.

Thus, it was agreed that the degree of error for the totals of the collected data was within  $\pm 1.708\%$ .

### 3. Results and discussions

In this investigation SBD30 + 1.5%DTBP+2%ARNP along with H<sub>2</sub> injection at the inlet manifold at a flow rate of 5–20 lpm in the variation of 5 lpm. This investigation mainly focused on the effect of H<sub>2</sub>, nanoparticle addition, and cetane number on the overall performance of a diesel engine under different loads.

#### 3.1. Combustion characteristics

##### 3.1.1. Ignition delay (ID)

Fig. 7 shows the variation of ID for diesel, SBD30 (30 % Spirogyra biodiesel blend), and SBD30 with the optimum concentrations of Di-Tertiary Butyl Peroxide (DTBP) and Algae Residual Carbon Nanoparticles (ARCNP), with various hydrogen flow rates. It was observed that the highest ID to diesel fuel tends to take place compared to fuel blends, majorly because the cetane number is smaller. On the other hand, SBD30 with 1.5 % DTBP, 2 % ARCNP, and hydrogen has an ID much lower than SBD30, primarily because of an improved cetane number due to the addition of ARCNP, hence fastening ignition. The conclusion of this research is in line with the conclusion of Vijay Kumar and Choudhary [8], who reported that the ID is decreased by adding hydrogen to the blends of microalgae biodiesel. They ascribed this to the fast ignition characteristics of hydrogen, which favored an earlier start-up time for combustion. Similarly, Mohite et al. [9] reported that the ID is reduced when a dual-fuel engine is operated with algae biodiesel and hydrogen as the fuel blend. This is because hydrogen being in gaseous form mixes quickly with the in-cylinder air, which in turn causes faster ignition. At all loads, the fuel blend with lowest ID is obtained with the SBD30 having 1.5 % DTBP, 2 % ARCNP and hydrogen flow rate of 20 LPM. This blend at full load ID was thereby 8.8° CA, significantly shorter than in diesel at 11.5° CA and in SBD30 at 10.3° CA. The results are in alignment with the trends depicted in the studies referenced above: where the synergistic effect between ARCNP and hydrogen addition to biodiesel blends considerably enhances combustion characteristics by shortening the ignition delay.

##### 3.1.2. Combustion duration (CD)

The CD for diesel, SDB30, and SBD30 + 1.5%DTBP+2%ARCNP + H<sub>2</sub> (5, 10, 15, and 20 lpm) blends are depicted in Fig. 8 with varying engine load. It is noticed from the figure that the blend SBD30 gives higher CD compared to diesel, SBD30 + 1.5%DTBP+2% ARCNP + H<sub>2</sub> (5, 10, 15, and 20 lpm) blends. This is due to low flame propagation and slow flame speed of the SBD30 during the combustion [6,31]. The CD for SBD30 is 38.6° CA which is 3.2 % lower than Diesel, and 5.3 %, 7.5 %, 10.6 %, and 11.2 % higher than SBD30 + 1.5%DTBP+2%ARCNP+5H<sub>2</sub>, SBD30 + 1.5%DTBP+2%ARCNP+10H<sub>2</sub>, SBD30 + 1.5%DTBP+2%ARCNP+15H<sub>2</sub>, and SBD30 + 1.5%DTBP+2%ARCNP+20H<sub>2</sub> respectively. Adding DTBP and ARCNP with H<sub>2</sub> leads to faster combustion resulting in low CD. These results are consistent with those documented by Mohite et al. [10] in an algae biodiesel-hydrogen dual fuel engine, wherein CD was also reduced due to the high propagation rate of flames through hydrogen, resulting in increasing the combustion speed. Similarly, Sindhu et al. [12] have revealed that microalgae biodiesel blends with hydrogen have shown reduced CD in altered diesel engines, because addition of hydrogen induces higher flame development and faster combustion and thus results in lowering of CD.

##### 3.1.3. Maximum cylinder pressure (MCP)

Fig. 9 depicts the variation of MCP for diesel, SDB30, and SBD30 + 1.5%DTBP+2%ARCNP + H<sub>2</sub> (5, 10, 15, and 20 lpm) mixes with various loads. SDB30 has a lower MCP than any of the other test fuels. However, the MCP of SBD30 + 1.5%DTBP+2%ARCNP+20H<sub>2</sub> is higher than that of other H<sub>2</sub> combinations. The greater MCP with 20 LPM H<sub>2</sub> is owing to the H<sub>2</sub>'s fast flame speed, which causes highly rapid combustion in a short CA, increasing MCP [32,33,34]. The MCP for 20 lpm H<sub>2</sub> is 3.48 %, 1.84 %, and 0.8 % greater than that of H<sub>2</sub> at flow rates of 5, 10, and 15 lpm. In an overall observation, SBD30 + 1.5%DTBP+2%ARCNP+15H<sub>2</sub> tends to a similar pattern of MCP

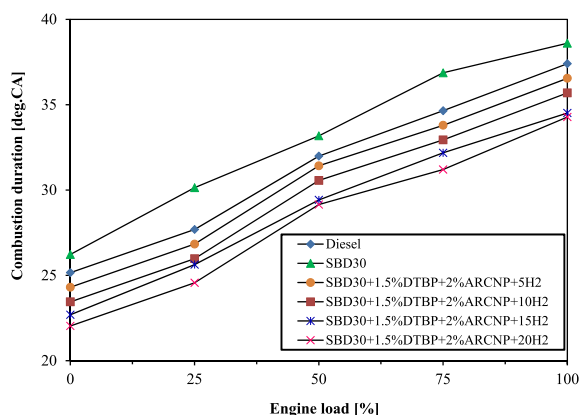


Fig. 8. CD vs Engine load.

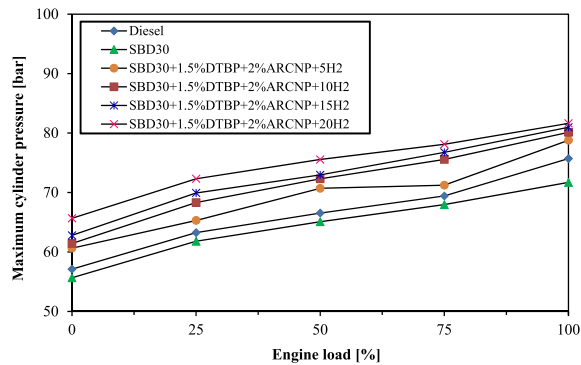


Fig. 9. MCP vs Engine load.

in comparison to SBD30 + 1.5%DTBP+2%ARCNP+20H<sub>2</sub>. The maximum MCP for test fuels at full load for Diesel, SBD30, SBD30 + 1.5%DTBP+2%ARCNP+5H<sub>2</sub>, SBD30 + 1.5%DTBP+2%ARCNP+10H<sub>2</sub>, SBD30 + 1.5%DTBP+2%ARCNP+15H<sub>2</sub>, and SBD30 + 1.5%DTBP+2%ARCNP+20H<sub>2</sub> are 75.7 bar, 71.7 bar, 78.8 bar, 80.1 bar, 81.0 bar, and 81.6 bar occurred at 11.5°CA, 10.3°CA, 9.9°CA, 9.5°CA, 9.2°CA, and 8.8°CA respectively. These results were in accord with Manigandan et al. [35], who reported an increase in MCP, significantly with the fast combustion induced by hydrogen addition in a corn biodiesel-hydrogen engine setup. Similarly, Barik et al. [15] stated that there was an increase of MCP in a hydrogen-diesel-diethyl ether dual-fuel engine due to enhanced combustion characteristics of hydrogen. Pullagura et al. [27] also reported that blending of graphene nanoplatelets and hydrogen with biodiesel diesel improved MCP, and this forms the basis of the notion that nanoparticle and hydrogen addition enhance combustion dynamics in the cylinder. The trends established in the current work correspond to analogous combustion enhancement mechanisms because of hydrogen and ARCNP, which result in higher pressure rise and MCP.

### 3.1.4. Cylinder pressure (CP) VS crank angle (CA)

The cylinder pressure of diesel, SBD30, SBD30 + 1.5%DTBP+2%ARCNP+5H<sub>2</sub>, SBD30 + 1.5%DTBP+2%ARCNP+10H<sub>2</sub>, SBD30 + 1.5%DTBP+2%ARCNP+15H<sub>2</sub>, and SBD30 + 1.5%DTBP+2%ARCNP+20H<sub>2</sub> for varying CA is depicted in Fig. 10. The peak cylinder pressure was observed for SBD30 with 1.5%DTBP and 2%ARCNP with 20 lpm H<sub>2</sub> which occurred at 8.83°CA aTDC. However, SBD30 gives the lowest peak cylinder pressure than other fuel blends which occurred at 10.2°CA aTDC. This reduction in peak cylinder pressure may be due to the slow-burning nature of SBD30 and the availability of lower free radicals in comparison to DTBP, ARCNP,

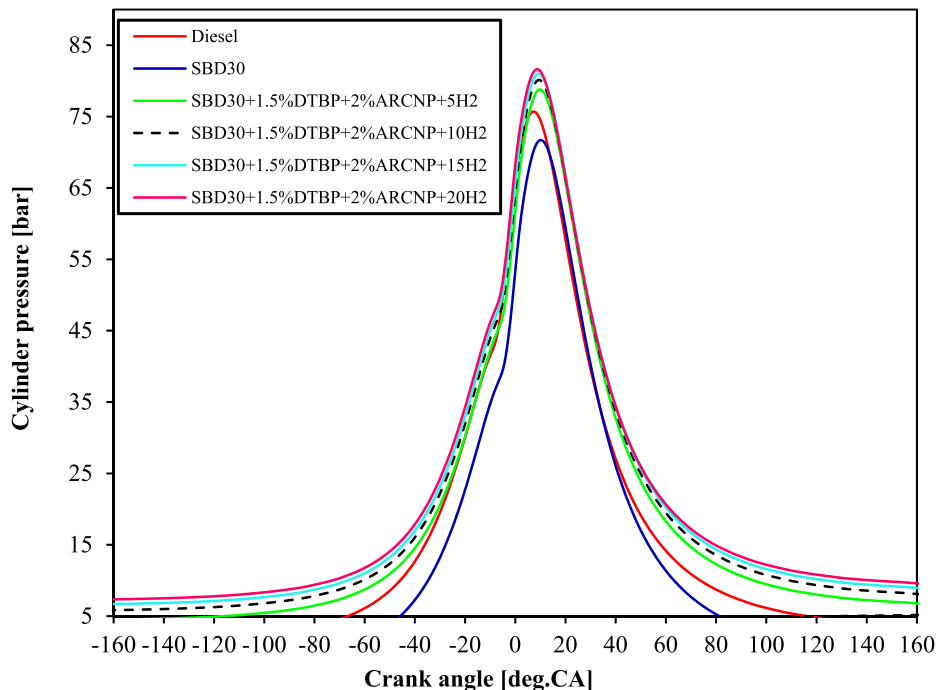


Fig. 10. Cylinder pressure vs °CA.

and  $H_2$  operation [13,29,36]. The maximum peak cylinder pressure for test fuels at full load for Diesel, SBD30, SBD30 + 1.5% DTBP+2%ARCNP+5 $H_2$ , SBD30 + 1.5%DTBP+2%ARCNP+10 $H_2$ , SBD30 + 1.5%DTBP+2%ARCNP+15 $H_2$ , and SBD30 + 1.5%DTBP+2%ARCNP+20 $H_2$  are 75.7 bar, 71.7 bar, 78.8 bar, 80.1 bar, 81.0 bar, and 81.6 bar at 11.52°CA, 10.27°CA, 9.91°CA, 9.55°CA, 9.19°CA and 8.83°CA respectively [37]. These results are in agreement with the conclusions arrived at by Barik et al. [15] which indicated that hydrogen enrichment within a dual-fuel diesel-diethyl ether system resulted in higher peak pressure because of quicker flame speed and faster ignition of hydrogen, thus causing an increase in pressure. Another similar conclusion is reported by Rajak et al. [13] concerning the increased cylinder pressure of hydrogen-enriched biodiesel blends since hydrogen accelerates combustion due to efficient fuel-air mixing along with better combustion kinetics. Another study done by Mohamed et al. [20] also validates that add-ons like ammonia with diesel increase the pressure inside the cylinder since combustion is more rapid for such add-ons. The above findings are also validated in the context of propensity towards addition of ARCNP, DTBP, and hydrogen to enhance the combustion process during higher peak pressure generation and shortening of the combustion duration process.

### 3.1.5. Heat release rate (HRR) and crank angle (CA)

The net HRR of diesel, SBD30 + 1.5%DTBP+2%ARCNP+5 $H_2$ , SBD30 + 1.5%DTBP+2%ARCNP+10 $H_2$ , SBD30 + 1.5%DTBP+2%ARCNP+15 $H_2$ , and SBD30 + 1.5%DTBP+2%ARCNP+20 $H_2$  for varying CA is illustrated in Fig. 11. SBD30 + 1.5%DTBP+2%ARCNP+20 $H_2$  gives a maximum HRR than that of other fuel blends. For SBD30 + 1.5%DTBP+2%ARCNP+15 $H_2$  is found to be 1.2 % lower than SBD30 + 1.5%DTBP+2%ARCNP+20 $H_2$ . In addition to this SBD30 offers the lowest HRR this is due to the low energy content in the SBD30 when compared to other fuel blends [9,38,39]. The maximum HRR for test fuels at full load for Diesel, SBD30, SBD30 + 1.5%DTBP+2%ARCNP+5 $H_2$ , SBD30 + 1.5%DTBP+2%ARCNP+10 $H_2$ , SBD30 + 1.5%DTBP+2%ARCNP+15 $H_2$ , and SBD30 + 1.5%DTBP+2%ARCNP+20 $H_2$  are 56.5 J/°CA, 55.4 J/°CA, 59.6 J/°CA, 60.9 J/°CA, 61.3 J/°CA, and 62 J/°CA respectively. Results are in agreement with Chaurasiya et al. [14], where hydrogen addition to the biodiesel blends accelerated HRR as hydrogen oxidizes rapidly and provides superior energy release within a short time span. Papparao and Murugan [40] have also established that a higher level of HRR was yielded through oxy-hydrogen gas addition as burning rates were increased by elevating the mixture's flame speed and hence, heat is produced quickly. Haleswadmath et al. [41] also reported a higher HRR when hydrogen was introduced in the engine manifold of a dual fuel setup utilizing biodiesel and producer gas. In all these studies, the high flame propagation speed of hydrogen and enhanced mixing with the air-fuel mixture enhanced the process of combustion thereby indicating quicker and efficient release of heat produced almost similar to the one in the current study for SBD30 with DTBP, ARCNP and hydrogen at various flow rates.

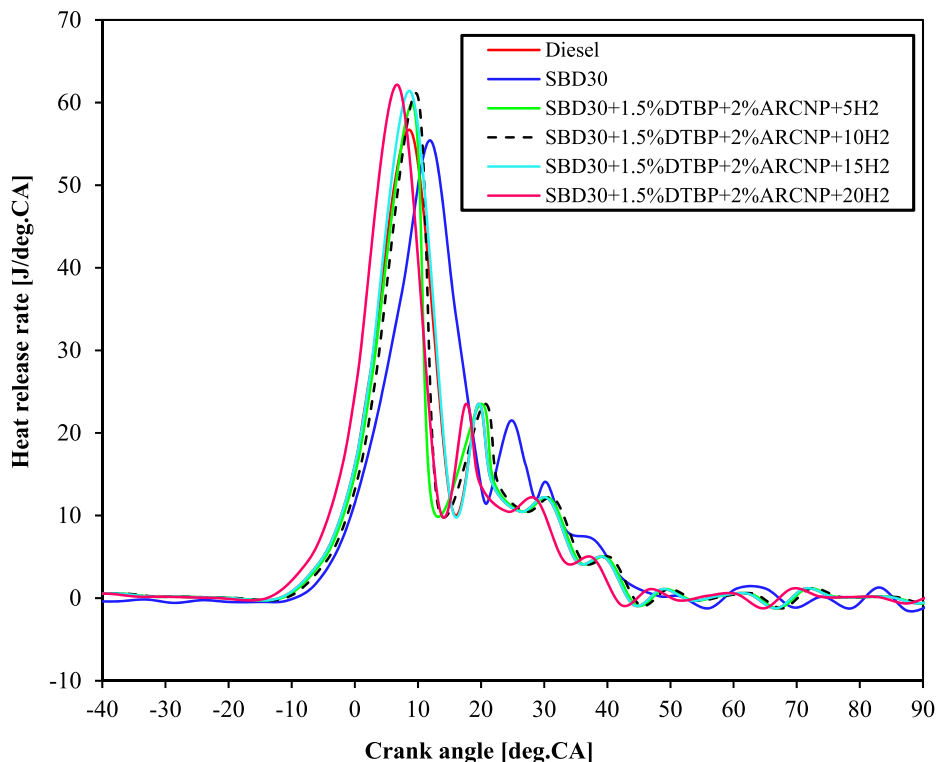


Fig. 11. HRR vs °CA.

### 3.2. Performance characteristics

#### 3.2.1. Brake-specific fuel consumption (BSFC)

Fig. 12 shows the variation of BSFC for varying engine load for test fuels diesel, SBD30, SBD30 + 1.5%DTBP+2%ARCNP+5H<sub>2</sub>, SBD30 + 1.5%DTBP+2%ARCNP+10H<sub>2</sub>, SBD30 + 1.5%DTBP+2%ARCNP+15H<sub>2</sub>, and SBD30 + 1.5%DTBP+2%ARCNP+20H<sub>2</sub>. The BSFC for SBD30 is higher when compared to other blends. This is due to the minimum energy content in the fuel in addition to this SBD30 makes a poor spray formation in comparison to diesel hence all the fuel does not take part in the combustion during the premixed combustion phase leading to loss of energy in the diffusion combustion and after burning phase [10,42]. The BSFC for H<sub>2</sub> operation is lower for all the test fuels in comparison to diesel and SBD30. This may be due to the addition of H<sub>2</sub> which may lead to rapid combustion and release of maximum heat energy making a completely combustible and end product leading to lower BSFC [14, 43]. The BSFC for SBD30 + 1.5%DTBP+2%ARCNP+15H<sub>2</sub> and SBD30 + 1.5%DTBP+2%ARCNP+20H<sub>2</sub> are almost identical. The addition of 20 lpm H<sub>2</sub> reduces the BSFC by 67.74 % more than that of SBD30. The BSFC for test fuels Diesel, SBD30, SBD30 + 1.5%DTBP+2%ARCNP+5H<sub>2</sub>, SBD30 + 1.5%DTBP+2%ARCNP+10H<sub>2</sub>, SBD30 + 1.5%DTBP+2%ARCNP+15H<sub>2</sub>, and SBD30 + 1.5%DTBP+2%ARCNP+20H<sub>2</sub> at full load was observed as 0.24, 0.31, 0.20, 0.16, 0.12, and 0.10 kg/kWh, correspondingly. These trends are in accordance with the findings of Mariam and Al-Dawody [21], who demonstrated the fact that the blends of microalgae biodiesel have higher BSFC comparing to diesel due to the low calorific value of the biodiesel, which in order to attain the same power, required an extra amount of fuel quantity. In the current experiment, the addition of hydrogen decreased BSFC. Bora et al. [30] also arrived at the conclusion that blends of hydrogen-enriched biodiesel displayed an essential reduction of BSFC in dual-fuel engine modes mainly as a result of the rapid burn-up of hydrogen and superior energy release. Kanth et al. [44] also support this trend where the BSFC might be drastically decreased because of hydrogen enrichment since the combustion characteristics were upgraded and the fuel consumptions were declined. Generally, these investigations confirm that the addition of hydrogen to the biodiesel blends had a lower BSFC in this study due to effective combustion and energy utilization.

#### 3.2.2. Brake thermal efficiency

The Brake Thermal Efficiency (BTE) of diesel, SBD30, SBD30 + 1.5%DTBP+2%ARCNP+5H<sub>2</sub>, SBD30 + 1.5%DTBP+2%ARCNP+10H<sub>2</sub>, SBD30 + 1.5%DTBP+2%ARCNP+15H<sub>2</sub>, and SBD30 + 1.5%DTBP+2%ARCNP+20H<sub>2</sub> fuel blends are depicted in Fig. 13. SBD30 + 1.5%DTBP+2%ARCNP+20H<sub>2</sub> gives the highest BTE in comparison to other test conditions throughout the load spectrum. It is also observed that the BTE for the H<sub>2</sub> operation was increasing trend up to 75 % load however it shows a mild declination at full load operation which may be due to induction of H<sub>2</sub> through the intake manifold may lead to a minute drop in volumetric efficiency leading to partial burning of the fuel. Which in turn reduces the BTE [7,11,45]. The BTE for SBD30 is lower compared to all other tested fuels due to the lower CV of SBD30. The BTE for diesel, SBD30, SBD30 + 1.5%DTBP+2%ARCNP+5H<sub>2</sub>, SBD30 + 1.5%DTBP+2%ARCNP+10H<sub>2</sub>, SBD30 + 1.5%DTBP+2%ARCNP+15H<sub>2</sub>, and SBD30 + 1.5%DTBP+2%ARCNP+20H<sub>2</sub> fuel blends are found to be 29.6 %, 23.5 %, 31.6 %, 33.2 %, 35.2 %, and 36.1 % at full load. Manigandan et al. [35], in a comparative study, proved similarly that the blending of hydrogen with nanoparticles had significantly improved BTE. Here was hydrogen's positive presence that enhanced the combustion process through an increase in flame speed, thereby efficiency. In Chetia et al. [33], an increase of BTE by the system augmented by hydrogen and with a mix of nanoparticles and biodiesel blends, which gives full combustion due to better ignition characteristics and heat release similar to the ongoing research work of additives ARCNP and DTBP. Rajak et al. [13] further validated this trend whereby hydrogen enriched blends with n-butanol and diethyl ester exhibited enhanced BTE because of improved combustion characteristics of hydrogen. The outcomes of these studies are in all directions that indicate the enhancement of BTE due to hydrogen enrichment in biodiesel blends is driven by better combustion and heat release. The current results are in agreement with this, where BTE of SBD30 was higher as compared to the base fuel for the samples considered after hydrogen addition.

#### 3.2.3. Exhaust gas temperature (EGT)

The EGT for diesel, SBD30, SBD30 + 1.5%DTBP+2%ARCNP + H<sub>2</sub> (5, 10, 15, and 20 lpm) fuel blends are depicted in Fig. 14 with

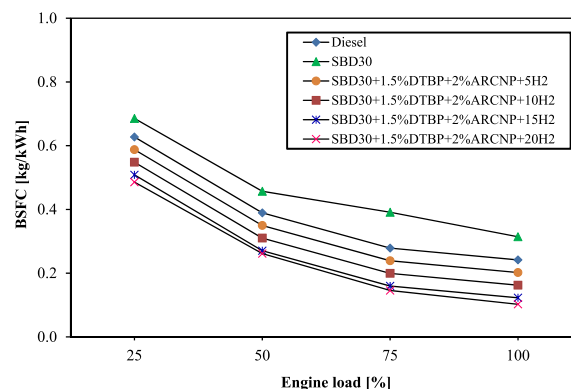


Fig. 12. BSFC vs Engine load.

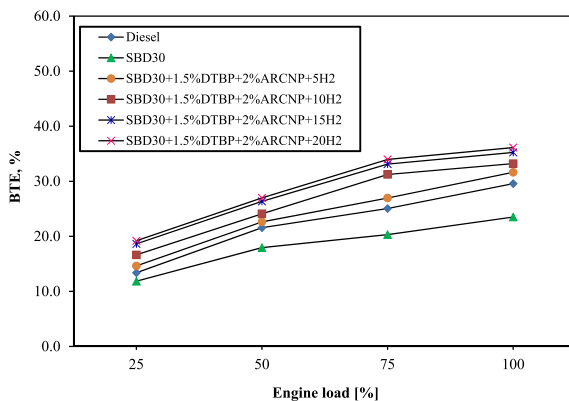


Fig. 13. BTE vs Engine load.

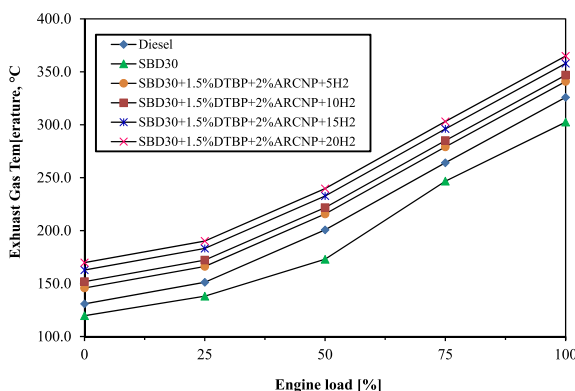


Fig. 14. EGT vs Engine load.

varying engine load. The EGT for all the test fuel increases with an increase in load this is due to an increase in cylinder temperature concerning an increase in load which may increase the local temperature leading to high EGT [30,46,47]. Among fuels tested in this investigation, SBD30 offers the lowest EGT however SBD30 + 1.5%DTBP+2%ARCNP+20H<sub>2</sub> which offers maximum EGT indicates that the H<sub>2</sub> fuel during its combustion produces high-temperature region as well as longer ID of gaseous fuel may lead to the release of maximum temperature at late combustion phase. The EGT of fuels tested Diesel, SBD30, SBD30 + 1.5%DTBP+2%ARCNP+5H<sub>2</sub>, SBD30 + 1.5%DTBP+2%ARCNP+10H<sub>2</sub>, SBD30 + 1.5%DTBP+2%ARCNP+15H<sub>2</sub>, and SBD30 + 1.5%DTBP+2%ARCNP+20H<sub>2</sub> are 325.9 °C, 302.4 °C, 340.9 °C, 346.9 °C and 364.9 °C respectively at full load. Mohamed F. Al-Dawody et al. [17] illustrated quite similar trends where hydrogen addition to Cladophora and Fucus green diesel blends resulted in increased EGT due to improved combustion characteristics, and therefore, the maximum temperature of combustion was achieved. They may have caused a higher

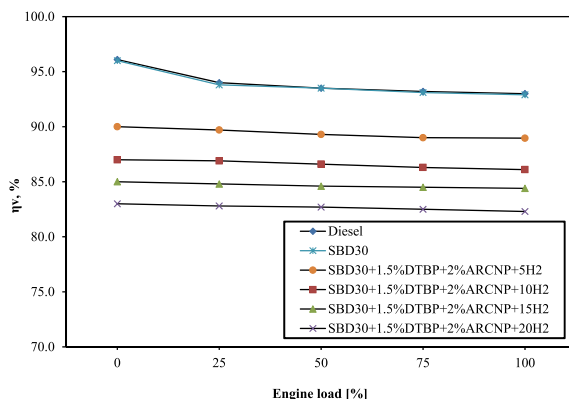


Fig. 15. Volumetric Efficiency vs Engine Load.

temperature, and the findings are well in agreement with the present study. In this present study, hydrogen-enriched blends were of high EGT values. Tosun and Özcanlı [48] also reported that EGT was found to have increased due to hydrogen enrichment in the diesel-soybean biodiesel blends with nanoparticles. It was attributed to the increased combustion efficiency besides faster flame propagation as responsible for EGT values. Similarly, Behera et al. [49] found that the high reactivity and energy released on combustion of hydrogen significantly increased the exhaust temperatures as observed with hydrogen-enriched blends in the present study. In tandem, these studies point out that hydrogen enrichment in biodiesel blends increases EGT largely due to mechanisms related to intensified combustion processes, extended ignition delays, and elevated flame temperatures. This corresponds to the trend shown for the SBD30 + 1.5%DTBP+2%ARCNP blends, especially with 20 LPM H<sub>2</sub> where the highest EGT was recorded.

### 3.2.4. Volumetric efficiency ( $\eta_v$ )

Fig. 15 shows the variation of volumetric efficiency ( $\eta_v$ , %) with load for diesel and other fuel blends. From the figure observed that as engine load increases, the volumetric efficiency decreases for all the test fuels. In the cases of diesel and SBD30, it was seen that there is a marginal reduction in the volumetric efficiency with the increase in load. This can be attributed to the fact that an increase in the engine temperature leads to an increase in the intake air temperature, reducing the air density and dropping the volumetric efficiency [42,43]. On the other hand, in dual fuel operation inducting H<sub>2</sub> through the intake manifold leads to a drop in volumetric efficiency throughout the load spectrum. This may be attributed to reduced air intake due to the supply of H<sub>2</sub>. A similar observation for a drop in volumetric efficiency in dual fuel operation with biogas was reported by the authors Barik et al. [15], Kanth et al. [31], and Pullagura et al. [26]. At H<sub>2</sub> flow rates of 5, 10, 15, and 20 LPM, the volumetric efficiency at full load was observed to be 89 %, 86.1 %, 84.4 %, and 82.3 % respectively. However, for diesel and SBD30 the volumetric efficiency was 93 % and 92.9 % which is much higher than the dual fuel operation.

## 3.3. Emission characteristics

### 3.3.1. CO emissions

Fig. 16 displays the variation of CO emission of diesel, SBD30, SBD30 + 1.5%DTBP+2%ARCNP+5H<sub>2</sub>, SBD30 + 1.5%DTBP+2%ARCNP+10H<sub>2</sub>, SBD30 + 1.5%DTBP+2%ARCNP+15H<sub>2</sub>, and SBD30 + 1.5%DTBP+2%ARCNP+20H<sub>2</sub> fuel blends with varying engine load. The CO emission for diesel is maximum compared to other test fuels because it is a mineral base and does not hold dissolved oxygen molecules which may lead to incomplete combustion releasing more CO emission [41,47]. However, H<sub>2</sub> dual fuel operation offers lower CO emission this is due to the availability of oxygen in SBD30 and DTBP as well and the use of DTBP leads to shorter ID giving sufficient time for the fuel to burn leading to low CO emission. The CO emission for SBD30 + 1.5%DTBP+2%ARCNP+15H<sub>2</sub> is found to be 31.4 % higher than SBD30 + 1.5%DTBP+2%ARCNP+20H<sub>2</sub> but 64.8 %, 48.5 %, 38.6 %, and 23.9 % lower than that of Diesel, SBD30, SBD30 + 1.5%DTBP+2%ARCNP+5H<sub>2</sub>, SBD30 + 1.5%DTBP+2%ARCNP+10H<sub>2</sub> at full load respectively. Xia et al. [32] similarly observed lower CO emissions for hydrogen-enriched biodiesel blends due to improved combustion and faster flame propagation, aided by nanoadditives that enhance oxidation. This aligns with the present study, where higher hydrogen enrichment in SBD30 blends reduced CO emissions. Barik et al. [15] reported emission of decreased CO in a dual-fuel engine using hydrogen and diesel-diethyl ether blends due to better combustion characteristics of hydrogen. Therefore, both studies verify the findings that hydrogen enrichment in biodiesel or a dual-fuel engine system significantly minimizes CO emissions, as observed in SBD30 + 1.5%DTBP+2%ARCNP + H<sub>2</sub> blends.

### 3.3.2. HC emission

The HC emission for test fuels diesel, SBD30, SBD30 + 1.5%DTBP+2%ARCNP+5H<sub>2</sub>, SBD30 + 1.5%DTBP+2%ARCNP+10H<sub>2</sub>, SBD30 + 1.5%DTBP+2%ARCNP+15H<sub>2</sub>, and SBD30 + 1.5%DTBP+2%ARCNP+20H<sub>2</sub> with varying engine load is portrayed in Fig. 17. The HC emission for diesel is maximum compared to other test fuels throughout the load spectrum this is due to the release of unburnt HC which does not take part in combustion, as well as the wall impingement of diesel, may lead to the release of higher HC and its burning in late combustion phase [15,50]. Among the H<sub>2</sub> DF operation, the HC emission is lower for SBD30 + 1.5%DTBP+2%ARCNP+20H<sub>2</sub>. For SBD30 + 1.5%DTBP+2%ARCNP+15H<sub>2</sub> the HC emission is 7.2 % higher than SBD30 + 1.5%DTBP+2%ARCNP+20H<sub>2</sub> but 38.8 %, 25.9 %, 22.6 %, and 12.7 % lower than other test fuels diesel, SBD30, SBD30 + 1.5%DTBP+2%ARCNP+5H<sub>2</sub>, SBD30 + 1.5%DTBP+2%ARCNP+10H<sub>2</sub> at full load respectively [44,34]. In dual-fuel and hydrogen-enriched biodiesel operation, Pullagura et al. [27] and Goyal et al. [28] minimize HC emission by enhancing combustion efficiency and better fuel-air mixing. The findings are in line with the present investigation, where SBD30 + 1.5%DTBP+2%ARCNP+20H<sub>2</sub> showed minimum HC emissions, as hydrogen enriches the combustion characteristics. Serin and Yıldızhan [51] also obtained decreased HC emission with hydrogen-enriched tea seed oil biodiesel blends. All the blends agree that HC emissions are reduced substantially with hydrogen enrichment, consistent with observations for SBD30 + 1.5%DTBP+2%ARCNP + H<sub>2</sub> blends, especially at higher levels of hydrogen enrichment.

### 3.3.3. NO emission

The NO emission of diesel, SBD30, SBD30 + 1.5%DTBP+2%ARCNP+5H<sub>2</sub>, SBD30 + 1.5%DTBP+2%ARCNP+10H<sub>2</sub>, SBD30 + 1.5%DTBP+2%ARCNP+15H<sub>2</sub>, and SBD30 + 1.5%DTBP+2%ARCNP+20H<sub>2</sub> fuel blends is illustrated in Fig. 18. The NO emission for the DF operation with H<sub>2</sub> and DTBP with ARCNP lead to an increase in NO emission than that of diesel and SBD30, this may be due to high-temperature combustion of H<sub>2</sub> leading to a reaction of nitrogen molecule with oxygen forming higher NO emission [52,39]. The NO emission for SBD30 + 1.5%DTBP+2%ARCNP+15H<sub>2</sub> is 4.9 % lower than SBD30 + 1.5%DTBP+2%ARCNP+20H<sub>2</sub> but it is 32.6 %, 16

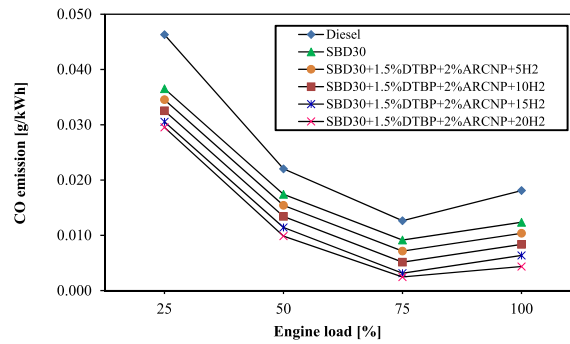


Fig. 16. CO emission vs Engine load.

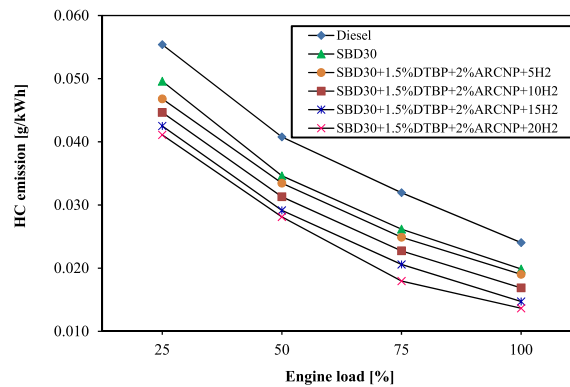


Fig. 17. HC emission vs Engine load.

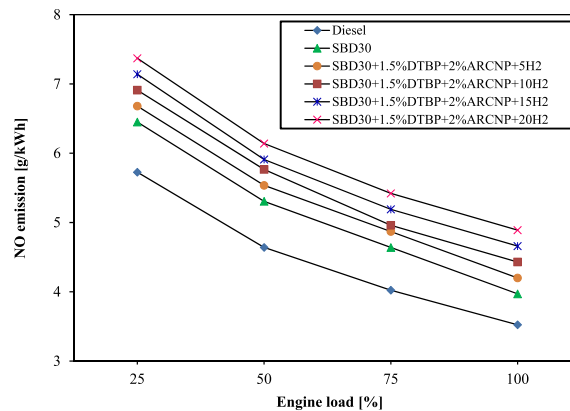


Fig. 18. NO emission vs Engine load.

17.37 %, 10.9 % and 5.19 % higher than Diesel, SBD30, SBD30 + 1.5%DTBP+2%ARCNP+5H<sub>2</sub>, SBD30 + 1.5%DTBP+2%ARCNP+10H<sub>2</sub> at full load respectively. Similar trends were reported by Halewadimath et al. [41] and Pinto et al. [50] in their works, which explained with the help of hydrogen addition that NO was increased with higher combustion temperatures. The same results were obtained in this work due to an increase in NO concentration for SBD30 + 1.5%DTBP+2%ARCNP + H<sub>2</sub> blends, especially with higher flow rates of hydrogen. Higher levels of NO were associated with improved combustion efficiency as well as temperature, specifically due to the impact of hydrogen. The two experiments suggest that hydrogen-rich fuel blends produce more NO because combustion is more complete and hotter.

### 3.3.4. Smoke emission

Fig. 19 displays the smoke emission of diesel, SBD30, SBD30 + 1.5%DTBP+2%ARCNP+5H<sub>2</sub>, SBD30 + 1.5%DTBP+2%

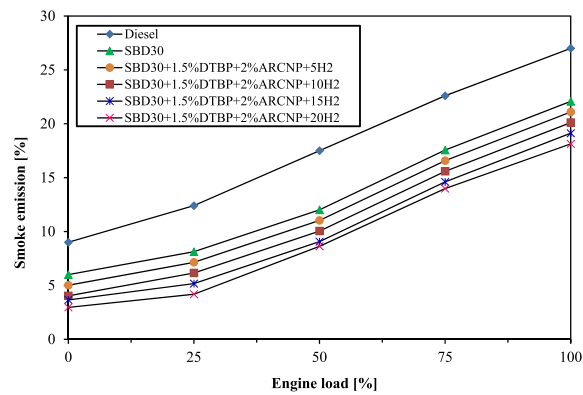


Fig. 19. Smoke emission vs Engine load.

ARCNP+10H<sub>2</sub>, SBD30 + 1.5%DTBP+2%ARCNP+15H<sub>2</sub>, and SBD30 + 1.5%DTBP+2%ARCNP+20H<sub>2</sub> test blends at varied engine loads. Smoke emission in the case of diesel is maximum because it does not have any oxygenated catalyst and it has a strong CH bond which leads to higher smoke emission. At full load, the smoke emission for SBD30 was 18.2 % lower than diesel. This is due to the renewable nature of SBD30 which does not contain any inorganic substances, additionally, it offers dissolved oxygen which helps to lower smoke emission during its combustion [53,38,54]. Among H<sub>2</sub> dual fuel operations with an increase in H<sub>2</sub> flow rate the smoke emission declines which are due to the clean burning nature of elemental H<sub>2</sub>. SBD30 + 1.5%DTBP+2%ARCNP+15H<sub>2</sub> gives 5.2 % higher smoke emission but 29.2 %, 13.4 %, 9.3 %, and 4.9 % lower than that of Diesel, SBD30, SBD30 + 1.5%DTBP+2%ARCNP+5H<sub>2</sub>, SBD30 + 1.5%DTBP+2%ARCNP+10H<sub>2</sub> at full load respectively. In other published work, Mohite et al. [10], Annamalai and Murgesan [11] and Sindhu et al. [12] also found hydrogen enrichment significantly lowered the smoke emissions. The bright burning characteristic of hydrogen, as well as its high flame speed, makes for a more complete combustion process, providing thereby less smoke emissions because of its intention. Similarly, within the present works, it was found that increasing hydrogen flow rates in SBD30 + 1.5%DTBP+2%ARCNP + H<sub>2</sub> blends led to a decrease in smoke emissions. Both studies assert that hydrogen addition in biodiesel blends, with algal and cork-based microalgal blends, is an effective way of lowering the smoke emissions, supporting the results of this current study.

#### 4. Conclusions

The experimental investigation on the combustion, performance, and emission characteristics of a diesel engine fueled with diesel, SBD30, and SBD30 + 1.5%DTBP+2%ARCNP with (5, 10, 15, and 20 lpm) flow rate of H<sub>2</sub> produced important results. The combination of SBD30 + 1.5%DTBP+2 % ARCNP fuel blend with a hydrogen flow rate of 15 LPM was determined to provide the optimum combustion efficiency, performance improvement and reduction in emission in the diesel engine. At this flow rate, ignition delay came down to 9.2° CA close to SBD30 (10.3°CA) and diesel (11.5°CA) but was faster, while combustion duration decreased by 10.6 % which consequently helped in completing the combustion process. They record a maximum cylinder pressure of 81.0 bar which is higher than both SBD30 at 71.7 bar and diesel at 75.7 bar; demonstrating enhanced combustion quality. Another set of parameters was enhanced as well; BTE became 35.2 %, much higher than 23.5 % in SBD30 and 29.6 % in diesel and BSFC was 0.12 kg/kWh which is 0.14 less than SBD with 61.3 % improvement. Emission amounts were also observed; CO levels were 38.6 % less than SBD30 while HC decreased by 25.9 % and smoke by 13.4 % illustrating the blends enhanced burn quality. While NO emissions rose, on account of heightened combustion temperatures, total emission characteristics will place this hydrogen-biodiesel and nanoparticle blend firmly within the broader category of cleaner fuels and superior to standard diesel. Nevertheless, the investigation suggests that SBD30 + 1.5% DTBP+2%ARCNP+15H<sub>2</sub> is a promising combination, demonstrating efficient combustion, improved performance, and reduced emissions.

##### 4.1. Future scope

As far as the future concern H<sub>2</sub> is considered as clean fuel having added advantages compared to other fuels. The clean combustion nature of H<sub>2</sub> opens many ways for advanced research in automotive sectors with the aid of artificial intelligence and sensor technology for the safe and efficient use of H<sub>2</sub>. Additionally, H<sub>2</sub> safe storage with metal hydrides for its long-term use also enlightens its successful application to on road and off-road combustion engines especially on dual fuel mode. In relation to this, the present research also enlightens the mechanism for large scale production of algae spirogyra biodiesel which may partially substitute the mineral based diesel.

##### 4.2. Future applications

The future prospects of the use of hydrogen-SBD dual-fuel engines are well appreciated due to clean combustion nature of H<sub>2</sub>,

especially in real-life applications such as for operating agricultural machinery, irrigation pumps and power generator sets to supply power in rural and off-grid regions. In addition, this technology can also be implemented for industrial machineries for process heating and power generation. This research comes under the category clean and sustainable energy that reflect to serve the need for society.

### CRedit authorship contribution statement

**S. Aravind:** Formal analysis. **Debabrata Barik:** Writing – original draft, Formal analysis. **Gandhi Pullagura:** Formal analysis. **Sreejesh S.R. Chandran:** Formal analysis. **Elumalai PV:** Resources. **Prabhu Paramasivam:** Methodology. **Dhinesh Balasubramanian:** Data curation. **Yasser Fouad:** Funding acquisition. **Manzoore Elahi M. Soudagar:** Conceptualization. **Md Abul Kalam:** Formal analysis. **Chan Choon Kit:** Supervision.

### Declaration of competing interest

The authors declare that they have no known competing financial interests or personal relationships that could have appeared to influence the work reported in this paper.

### Acknowledgement

The authors sincerely thank the Karpagam Academy of Higher Education (KAHE), Coimbatore, India, for providing facilities to carry out the research. The authors thank the Researchers Supporting Project number (RSPD2025R698), King Saud University, Riyadh, Saudi Arabia, for funding this research. The authors would like to acknowledge the management of Mepco Schlenk Engineering College, Sivakasi, Tamil Nadu, India for encouraging and supporting the research work.

### Appendix

**Table A1**

Instruments error analysis.

Instruments	Parameters measured	Range	Accuracy	Unreliability, %
Gas analyser	Exhaust emissions	NO 0–5000 ppm	±10 ppm	±0.2
		CO 0–10 %	±0.02 %	±0.15
		HC 0–10000 ppm	±20 ppm	±0.2
		CO <sub>2</sub> 0–20 %	±0.03 %	±0.2
Dynamometer	Brake power	0 - 100 Nm	±0.1 Nm	±0.2
Crank angle encoder	Crank position	0–720°	±0.2 °CA	±0.2
Speed sensor	Engine speed	0–10000 rpm	± 10 rpm	±0.1
Smoke meter	Smoke opacity	0–100 %	±0.1	±1
Burette	Fuel consumption	0–100 ml	±0.1 cc	±1
Pressure transducer	In-cylinder pressure	0–100 bar	±0.1 bar	±0.15

### Data availability

Data will be made available on request.

### References

- [1] L.T. Popoola, A.O. Agbo, U. Taura, A.S. Yusuff, Y.P. Asmara, O.A. Olagunju, O.M. Chima, Corrosion behavior of aluminum in fossil diesel fuel and biodiesel from chicken eggshell-alumina-catalyzed waste cooking oil, in: *Materials and Corrosion*, Wiley, 2024, <https://doi.org/10.1002/maco.202414510>.
- [2] S.K. Dash, D. Dash, P.K. Das, D. Barik, K.K. Dash, S.S.R. Chandran, M.S. Dennison, Investigation on the adjusting compression ratio and injection timing for a DI diesel engine fueled with policy-recommended B20 fuel. In *Discover Applied Sciences*, Springer Science and Business Media LLC 6 (8) (2024), <https://doi.org/10.1007/s42452-024-06076-w>.
- [3] A. Suresh, A.V. Babu, B. Balaji, P.S. Ranjit, Experimental investigation of NO<sub>x</sub> emission control using carbon nanotube additives and EGR configuration on CRDI engine fueled with ternary fuel, *Biofuels* 15 (10) (2024) 1315–1329, <https://doi.org/10.1080/17597269.2024.2366446>. Informa UK Limited.
- [4] Y. Chisti, Biodiesel from microalgae, *Biotechnol. Adv.* 25 (3) (2007) 294–306.
- [5] Y. Chisti, Biodiesel from microalgae beats bioethanol, *Trends Biotechnol.* 26 (3) (2008) 126–131.
- [6] E. Uludamar, Effect of hydroxy and hydrogen gas addition on diesel engine fuelled with microalgae biodiesel, *Int. J. Hydrogen Energy* 43 (38) (2018) 18028–18036.
- [7] P. Sharma, A. Chhillar, Z. Said, Z. Huang, V.N. Nguyen, P.Q.P. Nguyen, et al., Experimental investigations on efficiency and instability of combustion process in a diesel engine fueled with ternary blends of hydrogen peroxide additive/biodiesel/diesel, *Energy Sources, Part A Recovery, Util. Environ. Eff.* 44 (2022) 5929–5950, <https://doi.org/10.1080/15567036.2022.2091692>.
- [8] N. Vijay Kumar, A.K. Choudhary, A review on hydrogen and microalgae biodiesel fuel in IC engine, in: *AIP Conference Proceedings*, 2863, AIP Publishing, 2023, September, 1.

- [9] A. Mohite, B.J. Bora, P. Sharma, B.J. Medhi, D. Barik, D. Balasubramanian, D.N. Cao, Maximizing efficiency and environmental benefits of an algae biodiesel-hydrogen dual fuel engine through operational parameter optimization using response surface methodology, *Int. J. Hydrogen Energy* 52 (2024) 1395–1407.
- [10] A. Mohite, B.J. Bora, Ü. Ağbulut, P. Sharma, B.J. Medhi, D. Barik, Optimization of the pilot fuel injection and engine load for an algae biodiesel-hydrogen run dual fuel diesel engine using response surface methodology, *Fuel* 357 (2024) 129841.
- [11] B. Annamalai, P. Murugesan, The combined effect of hydrogen enrichment and exhaust gas recirculation on the combustion stability, performance and emissions of CI engine energized by algae biodiesel, *Int. J. Hydrogen Energy* 50 (2024) 524–546.
- [12] R. Sindhu, S.T. Prabhat, B.T. Hiep, A. Chinnathambi, S.A. Alharbi, Experimental assessment of cork-based *Botryococcus braunii* microalgae blends and hydrogen in modified multicylinder diesel engine, *Fuel* 359 (2024) 130468.
- [13] U. Rajak, P. Nashine, T.N. Verma, A. Pugazhendhi, Performance and emission analysis of a diesel engine using hydrogen-enriched n-butanol, diethyl ester and *Spirulina* microalgae biodiesel, *Fuel* 271 (2020) 117645.
- [14] P.K. Chaurasiya, U. Rajak, I. Veza, T.N. Verma, Ü. Ağbulut, Influence of injection timing on performance, combustion and emission characteristics of a diesel engine running on hydrogen-diethyl ether, n-butanol and biodiesel blends, *Int. J. Hydrogen Energy* 47 (41) (2022) 18182–18193.
- [15] D. Barik, B.J. Bora, P. Sharma, B.J. Medhi, D. Balasubramanian, R.L. Krupakaran, E.G. Varuvel, Exploration of the dual fuel combustion mode on a direct injection diesel engine powered with hydrogen as gaseous fuel in port injection and diesel-diethyl ether blend as liquid fuel, *Int. J. Hydrogen Energy* 52 (2024) 827–840.
- [16] C.B. Kumar, D.B. Lata, D. Mahto, Effect of addition of di-tert butyl peroxide (DTBP) on performance and exhaust emissions of dual fuel diesel engine with hydrogen as a secondary fuel, *Int. J. Hydrogen Energy* 46 (14) (2021) 9595–9612.
- [17] Mohamed F. Al-Dawody, Upendra Rajak, Ali A. Jazie, Khaled Al-Farhany, Gaurav Saini, Tikendra Nath Verma, Prerana Nashine, Production and performance of biodiesel from *Cladophora* and *Fucus* green diesel, *Sustain. Energy Technol. Assessments* 53 (Part D) (2022) 102761, <https://doi.org/10.1016/j.seta.2022.102761>. ISSN 2213-1388.
- [18] M.F. Al-Dawody, K.A. Al-Farhany, S. Allami, K.K.I. Al-Chlaihawi, W. Jamshed, M.R. Eid, A.A. Raezah, A. Amjad, S.M. El Din, Using oxy-hydrogen gas to enhance efficacy and reduce emissions of diesel engines, *Ain Shams Eng. J.* 14 (12) (2023) 102217.
- [19] Ali A. Jazie, Juma Haydari, Suhad A. Abed, Mohamed F. Al-Dawody, Hydrothermal liquefaction of *Fucus vesiculosus* algae catalyzed by H $\beta$  zeolite catalyst for Biocrude oil production, *Algal Res.* 61 (2022) 102596, <https://doi.org/10.1016/j.algal.2021.102596>. ISSN 2211-9264.
- [20] Mohamed F. Al-Dawody, Wisam Al-Obaidi, Emad D. Aboud, Mohammed A. Abdulwahid, Khaled Al-Farhany, Wasim Jamshed, Mohamed R. Eid, Zehba Raizah, Amjad Iqbal, Mechanical engineering advantages of a dual fuel diesel engine powered by diesel and aqueous ammonia blends, *Fuel* 346 (2023) 128398, <https://doi.org/10.1016/j.fuel.2023.128398>. ISSN 0016-2361.
- [21] Mariam E. Murad, Mohamed F. Al-Dawody, Effect of microalgae biodiesel blending on diesel engine characteristics, *Heat Transfer* 51 (7) (2022) 6616–6640, <https://doi.org/10.1002/htj.22615>.
- [22] M.E. Murad, M.F. Al-Dawody, Effect of microalgae biodiesel blending on diesel engine characteristics, *Heat Transfer* 51 (7) (2022) 6616–6640.
- [23] N.H. Hamza, M.F. Al-Dawody, K.A. Al-Farhany, et al., Impact of using different biofuels on the characteristics of turbocharged diesel engine: an application towards mechanical engineering, *Environ. Dev. Sustain.* (2023), <https://doi.org/10.1007/s10668-023-03923-5>.
- [24] N.H. Hamza, M.F. Al-Dawody, K.A. Al-Farhany, U. Rajak, T.N. Verma, Impact of using different biofuels on the characteristics of turbocharged diesel engine: an application towards mechanical engineering, *Environ. Dev. Sustain.* (2023) 1–19.
- [25] H.-R. Wei, M.E.M. Soudagar, N.N. Bhooshanam, V.V. Upadhyay, N. Kumar, R. Srinivasan, I. Hossain, S. Al Obaid, S.A. Alharbi, Influences of cerium oxide on Chlorophyta growth and utilized as feedstock for hydrogen generation: performance study, in: *International Journal of Hydrogen Energy*, Elsevier BV, 2024, <https://doi.org/10.1016/j.ijhydene.2024.10.328>.
- [26] G. Pullagura, J.R. Bikkavolu, S. Vadapalli, P.V.V. Siva, K.R.R. Chebattina, D. Barik, B.J. Bora, Amplifying performance attributes of biodiesel–diesel blends through hydrogen infusion and graphene oxide nanoparticles in a diesel engine, *Clean Technol. Environ. Policy* (2024) 1–23.
- [27] G. Pullagura, V.S.P. Vanthala, S. Vadapalli, J.R. Bikkavolu, D. Barik, P. Sharma, B.J. Bora, Enhancing performance characteristics of biodiesel-alcohol/diesel blends with hydrogen and graphene nanoplatelets in a diesel engine, *Int. J. Hydrogen Energy* 50 (2024) 1020–1034.
- [28] D. Goyal, T. Goyal, S.K. Mahla, G. Goga, A. Dhir, D. Balasubramanian, K. Brindhadevi, Application of Taguchi design in optimization of performance and emissions characteristics of n-butanol/diesel/biogas under dual fuel mode, *Fuel* 338 (2023) 127246.
- [29] M. Vijayaragavan, B. Subramanian, S. Sudhakar, L. Natrayan, Effect of induction on exhaust gas recirculation and hydrogen gas in CI engine with simarouba oil in DF mode, *Int. J. Hydrogen Energy* 47 (88) (2022) 37635–37647.
- [30] B.J. Bora, P. Sharma, B. Deepanraj, Ü. Ağbulut, Investigations on a novel fuel water hyacinth biodiesel and Hydrogen-Powered engine in DF Model: optimization with I-optimal design and desirability, *Fuel* 345 (2023) 128057.
- [31] S. Kanth, S. Debbarma, B. Das, Effect of hydrogen enrichment in the intake air of diesel engine fuelled with honge biodiesel blend and diesel, *Int. J. Hydrogen Energy* 45 (56) (2020) 32521–32533.
- [32] C. Xia, K. Brindhadevi, A. Elfasakhany, M. Alsehli, S. Tola, Performance, combustion and emission analysis of castor oil biodiesel blends enriched with nano additives and hydrogen fuel using CI engine, *Fuel* 306 (2021) 121541.
- [33] B. Chetia, S. Debbarma, B. Das, An experimental investigation of hydrogen-enriched and nanoparticle blended waste cooking biodiesel on diesel engine, *Int. J. Hydrogen Energy* 49 (2024) 23–37.
- [34] B. Duraisamy, E.G. Varuvel, S. Palanichamy, B. Subramanian, M.J. Stanley, D.K. Madheswaran, Impact of hydrogen addition on diesel engine performance, emissions, combustion, and vibration characteristics using a *Prosopis Juliflora* methyl ester-decanol blend as pilot fuel, *Int. J. Hydrogen Energy* 75 (2024) 12–23.
- [35] S. Manigandan, V.K. Ponnusamy, P.B. Devi, S.A. Oke, Y. Sohret, S. Venkatesh, P. Gunasekar, Effect of nanoparticles and hydrogen on combustion performance and exhaust emission of corn blended biodiesel in compression ignition engine with advanced timing, *Int. J. Hydrogen Energy* 45 (4) (2020) 3327–3339.
- [36] S.K. Nayak, H.S. Le, J. Kowalski, B. Deepanraj, X.Q. Duong, T.H. Truong, V.D. Tran, D.N. Cao, P.Q.P. Nguyen, Performance and emission characteristics of diesel engines running on gaseous fuels in dual-fuel mode, *Int. J. Hydrogen Energy* 49 (2024) 868–909.
- [37] H.B. Aditya, M. Aziz, Prospect of hydrogen energy in Asia-Pacific: a perspective review on techno-socio-economy nexus, *Int. J. Hydrogen Energy* 46 (71) (2021) 35027–35056.
- [38] Z. Qin, F. Liu, H. Zhang, X. Wang, C. Yin, W. Weng, Z. Han, Study of hydrogen injection strategy on fuel mixing characteristics of a free-piston engine, *Case Stud. Therm. Eng.* 56 (2024) 104279.
- [39] T. Gammaidoni, A. Miliozzi, J. Zembi, M. Battistoni, Hydrogen mixing and combustion in an SI internal combustion engine: CFD evaluation of premixed and DI strategies, *Case Stud. Therm. Eng.* 55 (2024) 104072.
- [40] J. Paparao, S. Murugan, DF diesel engine run with injected pilot biodiesel-diesel fuel blend with inducted oxy-hydrogen (HHO) gas, *Int. J. Hydrogen Energy* 47 (40) (2022) 17788–17807.
- [41] S.S. Halewadamath, N.R. Banapurmath, V.S. Yaliwal, M.G. Prasad, S.S. Jalihal, M.E.M. Soudagar, H. Yaqoob, M.A. Mujtaba, K. Shahapurkar, M.R. Safaei, Effect of manifold injection of hydrogen gas in producer gas and neem biodiesel fueled CRDI DF engine, *Int. J. Hydrogen Energy* 47 (62) (2022) 25913–25928.
- [42] A.F. Fareed, A.S. El-Shafay, M.A. Mujtaba, F. Riaz, M.S. Gad, Investigation of waste cooking and castor biodiesel blends effects on diesel engine performance, emissions, and combustion characteristics, *Case Stud. Therm. Eng.* 60 (2024) 104721.
- [43] B.N. Behera, T.K. Hotta, Experimental investigation of performance, emission, and combustion characteristics of a variable compression ratio engine using waste cooking vegetable oils blended with diesel, *Case Stud. Therm. Eng.* 58 (2024) 104394.
- [44] S. Kanth, S. Debbarma, B. Das, Experimental investigations on the effect of fuel injection parameters on diesel engine fuelled with biodiesel blend in diesel with hydrogen enrichment, *Int. J. Hydrogen Energy* 47 (83) (2022) 35468–35483.
- [45] M. Sonachalam, R. Jayaprakash, V. Manieniyani, M.S. Murthy, M.G.M. Johar, S. Sivaprakasam, M. Warimani, N. Kumar, A. Majdi, M. Alsibih, S. Islam, Impact of injection pressure on a dual-fuel engine using acetylene gas and microalgae blends of *Chlorella protothecoides*, *Case Stud. Therm. Eng.* 60 (2024) 104653.

- [46] N. Gültekin, M. Ciniviz, Experimental investigation of the effect of hydrogen ratio on engine performance and emissions in a CI SC engine with electronically controlled hydrogen-diesel DF system, *Int. J. Hydrogen Energy* 48 (66) (2023) 25984–25999.
- [47] A.R. Palanivelrajan, R. Manimaran, S. Manavalla, T.Y. Khan, N. Almakayeel, M. Feroskhan, Performance and emission characteristics of biogas fuelled dual fuel engine with waste plastic oil as secondary fuel, *Case Stud. Therm. Eng.* 57 (2024) 104337.
- [48] E. Tosun, M. Özcanlı, Hydrogen enrichment effects on performance and emission characteristics of a diesel engine operated with diesel-soybean biodiesel blend with nanoparticle addition, *Engineering Science and Technology, an International Journal* 24 (3) (2021) 648–654.
- [49] M. Behera, P.R. Behera, P.P. Bhuyan, L. Singh, B. Pradhan, Algal nanoparticles and their antibacterial activity: current research status and future perspectives, *Drugs and Drug Candidates* 2 (3) (2023) 554–570.
- [50] G.M. Pinto, T.A.Z. de Souza, R.B.R. da Costa, L.F.A. Roque, G.V. Frez, C.J.R. Coronado, Combustion, performance and emission analyses of a CI engine operating with renewable diesel fuels (HVO/FARNESANE) under DF mode through hydrogen port injection, *Int. J. Hydrogen Energy* 48 (51) (2023) 19713–19732.
- [51] H. Serin, Ş. Yıldızhan, Hydrogen addition to tea seed oil biodiesel: performance and emission characteristics, *Int. J. Hydrogen Energy* 43 (38) (2018) 18020–18027.
- [52] N. Khatri, K.K. Khatri, Hydrogen enrichment on diesel engine with biogas in DF mode, *Int. J. Hydrogen Energy* 45 (11) (2020) 7128–7140.
- [53] M. Akcay, I.T. Yilmaz, A. Feyzioglu, The influence of hydrogen addition on the combustion characteristics of a common-rail CI engine fueled with waste cooking oil biodiesel/diesel blends, *Fuel Process. Technol.* 223 (2021) 106999.
- [54] R. Li, Y. Zhang, X. Chen, D. Wang, Q. Liu, X. Liu, Experimental study on the combustion characteristics of hydrogen/ammonia blends in oxygen, *Case Stud. Therm. Eng.* (2024) 104732.